TI 2000-015/1
Tinbergen Institute Discussion Paper

Bifurcation Routes to Volatility Clustering

Andrea Gaunersdorfer
Cars Hommes
Florian O.O. Wagener

Tinbergen Institute
The Tinbergen Institute is the institute for economic research of the Erasmus Universiteit Rotterdam, Universiteit van Amsterdam and Vrije Universiteit Amsterdam.

Tinbergen Institute Amsterdam
Keizersgracht 482
1017 EG Amsterdam
The Netherlands
Tel.: +31.(0)20.5513500
Fax: +31.(0)20.5513555

Tinbergen Institute Rotterdam
Burg. Oudlaan 50
3062 PA Rotterdam
The Netherlands
Tel.: +31.(0)10.4088900
Fax: +31.(0)10.4089031

Bifurcation Routes to Volatility Clustering

Andrea Gaunersdorfer

Department of Business Studies
University of Vienna

Cars H. Hommes
Florian O. O. Wagener

Center for Nonlinear Dynamics in Economics and Finance
University of Amsterdam

September 5, 2000

Abstract

A simple asset pricing model with two types of adaptively learning traders, fundamentalists and technical analysts, is studied. Fractions of these trader types, which are both boundedly rational, change over time according to evolutionary learning, with technical analysts conditioning their forecasting rule upon deviations from a benchmark fundamental. Volatility clustering arises endogenously in this model. Two mechanisms are proposed as an explanation. The first is coexistence of a stable steady state and a stable limit cycle, which arise as a consequence of a so-called Chenciner bifurcation of the system. The second is intermittency and associated bifurcation routes to strange attractors. Both phenomena are persistent and occur generically in nonlinear multi-agent evolutionary systems.

JEL classification: E32, G12, D84

Keywords: multi-agent systems, bounded rationality, evolutionary learning, bifurcation and chaos, coexisting attractors

Acknowledgements. This research was supported by the Austrian Science Foundation (FWF) under grant SFB#010 ('Adaptive Information Systems and Modelling in Economics and Management Science.') and by the Netherlands Organization for Scientific Research (NWO) under a NWO-MaG Pionier grant.

Corresponding author: Cars Hommes, Center for Nonlinear Dynamics in Economics and Finance (CeNDEF), University of Amsterdam, Roetersstraat 11, NL-1018 WB Amsterdam, The Netherlands, e-mail: hommes@fee.uva.nl

Contents

1 Introduction

Modern finance is based on the concept of rational expectations. As a consequence financial markets are considered to be efficient in the sense that past prices cannot help in predicting future prices. This view is known as the efficient market hypothesis (EMH). There has been a long debate about the EMH. In particular, there is empirical evidence that many so-called 'stylized facts' observed in financial time series cannot solely be explained by fundamentals, but that markets have internal dynamics of their own.

One of the most important 'stylized facts' is volatility clustering. Whereas changes in asset prices themselves appear to be unpredictable, the magnitude of those changes seems to be predictable in the sense that large changes tend to be followed by large changes – either positive or negative – and small changes tend to be followed by small changes. Asset price fluctuations are thus characterized by episodes of high volatility, with large price changes, irregularly interchanged by episodes of low volatility, with small price changes. Mandelbrot (1963) first discovered this phenomenon in commodity prices. Since the pioneering work of Engle (1982) and Bollerslev (1986) on autoregressive conditional heteroskedastic (ARCH) models and their generalization to GARCH models, volatility clustering has been shown to be present in a wide variety of financial assets including stocks, market indices and exchange rates.

In empirical work, volatility clustering is usually modeled by a *statistical* model, such as the familiar (G)ARCH model or one of its extensions. Although these models are useful as a statistical description of the data, they do not offer a structural explanation of why volatility clustering is present in so many financial time series. Rather the statistical models postulate that volatility clustering has an exogenous source and is for example caused by the clustered arrival of random 'news' about economic fundamentals.

A recent branch of literature, including for example Arthur et al. (1997), Brock and Hommes (1997, 1998), Farmer (2000), Gaunersdorfer and Hommes (2000), LeBaron (2000), LeBaron et al. (1999), Lux (1995) and Lux and Marchesi (1999a,b), has offered a structural explanation of the phenomenon of volatility clustering by multi-agent systems, where financial markets are viewed as complex evolutionary systems between competing boundedly rational trading strategies. In these multi-agent systems two important classes of traders can be distinguished, fundamentalists and technical analysts, that have different trading strategies and expectations about future prices of a risky asset. The fundamentalists believe that prices will move towards its fundamental rational expectations (RE) value, as given by the expected discounted sum of future dividends. In contrast, the technical analysts observe past prices and try to extrapolate historical patterns. Volatility clustering arises as an endogenous phenomenon, caused or amplified by the trading process itself through the interaction between fundamentalists and technical analysts. The multi-agent systems are characterized by an irregular switching between phases of low volatility, where fundamentalists dominate the market and prices move close to the RE fundamental price, and phases of high volatility, where the market is dominated by

technical trading with prices deviating from the fundamental price. Volatility clustering thus becomes an endogenous phenomenon driven by news about economic fundamentals, but amplified by heterogeneity and adaptive learning.

This paper investigates asset price fluctuations in a simple *adaptive belief system* introduced by Gaunersdorfer and Hommes (2000), extending the present discounted value asset pricing model with heterogeneous beliefs of Brock and Hommes (1998). There are only two trader types: fundamentalists, who believe that prices will move in the direction of the 'fundamental value', and trend followers or chartists, who extrapolate the latest observed price change. The fractions of the two different trader types change over time according to evolutionary fitness, as measured by utility from realized profits or, equivalently, forecasting accuracy in the recent past. Chartists, however, also condition their forecasting rule upon price deviations from the RE fundamental price. Gaunersdorfer and Hommes (2000), henceforth GH (2000), have investigated the time series properties of this adaptive belief system buffeted with dynamic noise. They showed that the evolutionary dynamics is characterized by unpredictable asset price returns, with almost no significant autocorrelations, and at the same time by predictable squared returns, with significant and slowly decaying autocorrelation coefficients. Put differently, the simple adaptive belief system generates simultaneously unpredictable returns and volatility clustering, and provides a structural explanation of the first and second moments of the returns distribution of asset prices. The present paper shows that two fundamentally important concepts explain the endogenous occurrence of volatility clustering: intermittency and coexistence of attractors.

The phenomenon of *intermittency*, as introduced by Pomeau and Manneville (1980), occurs when asset price fluctuations are moving on a strange, chaotic attractor characterized by phases of almost periodic fluctuations irregularly interrupted by sudden bursts of erratic fluctuations. In the evolutionary learning model studied here intermittency is characterized by close to the RE fundamental steady state fluctuations, suddenly interrupted by price deviations from the fundamental triggered by technical trading. Recent mathematical results on homoclinic bifurcations have shown that strange attractors are persistent in the sense that they typically occur for a positive Lebesgue measure set (i.e. a set of positive probability) of parameter values, see e.g. Palis and Takens (1993) for a mathematical treatment; recent economic applications include the overlapping generations economy in de Vilder (1996) and the 'hog cycle' or cobweb model with evolutionary learning in Brock and Hommes (1997a).

The second phenomenon naturally suited to describe volatility clustering is *coexistence of attractors.* In particular, our evolutionary model exhibits coexistence of a stable steady state and a stable limit cycle due to a so-called *Chenciner* or *degenerate Hopf bifurcation.* When buffeted with dynamic noise, irregular switching occurs between close to fundamental steady state fluctuations, where the market is dominated by fundamentalists, and large amplitude price fluctuations, where the market is dominated by chartists. It is important to note that both, intermittency and coexistence of attractors, are *persistent* phenomena, which are by no means special to our evolutionary system, but occur naturally in nonlinear

dynamic models, and moreover are robust with respect to and sometimes even reinforced by dynamic noise. In particular, coexistence of attractors is a structurally stable phenomenon, occurring for an open set of parameter values. The Chenciner bifurcation has codimension two, implying that it is a generic feature in nonlinear systems with two or more parameters. We conjecture that both mechanisms proposed here, intermittency and coexistence of attractors, are also relevant to other computationally oriented nonlinear evolutionary multi-agent systems such as the Santa Fe Artifical stock market and other references cited above.

An important critique from 'rational expectations finance' upon heterogeneous agent models using simple habitual rule of thumb forecasting rules is that 'irrational' traders will *not* survive in the market. For example, Friedman (1953) argues that irrational speculative traders would be driven out of the market by rational traders, who would trade against them by taking infinitely long opposite positions, thus driving prices back to fundamentals. In an efficient market, 'irrational' speculators would simply lose money and disappear from the market.

However, for example, De Long et al. (1990) have shown that a constant fraction of noise traders may on average earn higher expected returns than rational or smart money traders, and may survive in the market with positive probability.[1] Brock and Hommes (1997a,b, 1998, 1999), henceforth BH, have also discussed this point extensively in a series of papers, and stress the fact that in an evolutionary framework technical analysts are not 'irrational', but they are in fact *boundedly rational*, since in periods when prices deviate from the RE fundamental price, chartists make better forecasts and earn higher profits than fundamentalists. Speculative deviations from the fundamental price may in fact be triggered by short run profit opportunities for chartists. On average, technical analysts and fundamentalists may earn approximately equal profits, so that in general fundamentalists can *not* drive chartists out of the market. See the survey in Hommes (2000) for an extensive discussion of these points. See also Grandmont (1998), Evans and Honkapohja (1998), and Sargent (1993, 1999) for related work on adaptive learning and motivation of bounded rationality.[2] In related empirical work Brock et al. (1992) have shown that simple technical trading rules applied to the Dow Jones Index may yield positive returns, suggesting extra structure above and beyond the EMH fundamental.

The paper is organized as follows. Section 2 describes the asset pricing model with fundamentalists and chartists. Section 3 presents a stability analysis of the fundamental steady state and bifurcations of codimension one and two. Section 4 contains a numerical analysis of typical bifurcation routes, wheras section 5 focusses on complicated, chaotic dynamics. Section 6 discusses the effect of noise on these systems. Finally, section 7 concludes.

[1] An early example of a heterogeneous agent model is Zeeman (1974); other more recent examples include Frankel and Froot (1988), Kirman (1991), Chiarella (1992) and Brock (1993).

[2] Timmerman (1993, 1996), for example studies, adaptive learning and its role for generating excess volatility in asset pricing models. Our evolutionary approach is also related to reinforcement learning in evolutionary game theory as e.g. in Börgers and Sarin (1997).

In an appendix we present so-called normal form computations of the Hopf bifurcation underlying the numerical computations of the Chenciner bifurcation points.

2 The model

We briefly recall the asset pricing model with heterogeneous beliefs introduced in BH (1997b, 1998, 1999), see also Brock (1997), Gaunersdorfer (2000a), and GH (2000). Agents trade in a market with one risky and one risk-free asset. The risk-free asset is completely elastically supplied at a gross return $R > 1$. p_t denotes the price (ex-dividend) of the risky asset and $\{y_t\}$ the (stochastic) dividend process. The dynamics of wealth of investor type h is described by

$$\tilde{W}_{h,t+1} = RW_{ht} + \tilde{R}_{t+1} z_{ht},$$

where z_{ht} is the number of shares of the risky asset purchased at time t and $\tilde{R}_{t+1} = \tilde{p}_{t+1} + \tilde{y}_{t+1} - Rp_t$ is the excess return per share. Variables carrying tildes denote random variables. Let E_t and V_t denote conditional expectation and conditional variance based on a publically available information set $\mathcal{F}_t$, such as past prices and dividends, and let E_{ht} and V_{ht} denote the 'beliefs' or forecasts of investor type h about these conditional expectation and variance.

Equilibrium

Assuming that investors are myopic mean-variance maximizers, the demand for shares z_{ht} by type h solves

$$\max\{E_{ht}\tilde{W}_{h,t+1} - \frac{a}{2} V_{ht}\tilde{W}_{t+1}\}, \quad \text{i.e.} \quad z_{ht} = \frac{E_{ht}\tilde{R}_{t+1}}{aV_{ht}\tilde{R}_{t+1}}. \tag{1}$$

Here the nonnegative parameter a characterizes risk aversion. Let z_{st} and n_{ht} denote respectively the supply of shares per investor and the fraction of investors of type h at time t. Equilibrium of supply and demand implies

$$\sum_h n_{ht} z_{ht} = z_{st}. \tag{2}$$

Assuming constant supply of outside shares over time we may stick to the (equivalent) special case $z_{st} \equiv 0$.[3] Further, we assume that dividends are independently and identically distributed (iid), in particular, $E_t\tilde{y}_{t+1} \equiv y^*$.

Beliefs

In the case where there is only one type of traders the equilibrium equation (2) reduces to

$$Rp_t = E_t\tilde{p}_{t+1} + y^*.$$

[3] In the general case $z_{st} = \text{const}$ one can introduce a risk adjusted dividend $y^{\#}_{t+1} = y_{t+1} - a\sigma^2 z^s$, see Brock (1997).

In the standard case $R > 1$ there is only one solution $p_t^* \equiv p^* = y^*/(R-1)$ that satisfies the 'no bubbles' condition $\lim_{t\to\infty} E\tilde{p}_t^*/R^t = 0$. This price, given as the discounted sum of expected future dividends, would prevail in a perfectly rational world and will be called the *fundamental price*.

We make some simplifying assumptions concerning the beliefs:

A1 The beliefs about future prices and dividends are assumed to be of the form

$$E_{ht}(\tilde{p}_{t+1} + \tilde{y}_{t+1}) = E_t(\tilde{p}_{t+1}^*) + y^* + f_h(p_{t-1}, \ldots, p_{t-L}) = Rp_t^* + f_h(p_{t-1}, \ldots, p_{t-L}),$$

where f_h is some *deterministic* function of past prices describing the beliefs of traders about price deviations from the fundamental value. Further, this assumption implies that investors have homogeneous beliefs about future dividends $E_{ht}(\tilde{y}_{t+1}) = E_t(\tilde{y}_{t+1}) = y^*$. Hence all traders are able to derive the fundamental price p_t^*.

A2 The beliefs about conditional variances of the excess returns are assumed to be of the form

$$V_{ht}\tilde{R}_{t+1} = V_t\tilde{R}_{t+1} \equiv \sigma^2, \quad \forall h, t.$$

That is, beliefs about conditional variances are the same for all types and constant over time.[4]

We consider a model with two simple belief types,

$$E_{1,t+1} \equiv p_{1,t+1}^e = p^* + v(p_{t-1} - p^*), \qquad 0 \le v \le 1 \tag{3}$$
$$E_{2,t+1} \equiv p_{2,t+1}^e = p_{t-1} + g(p_{t-1} - p_{t-2}), \quad g \in \mathbb{R}. \tag{4}$$

Trader type 1 are 'fundamentalists', believing that tomorrow's price will move in the direction of the fundamental price p^* by a factor v. Trader type 2 derive their beliefs from price histories. If $g > 0$ these traders are trend followers, extrapolating the latest observed price change, if $g < 0$ they are contrarians. Given our assumptions, the equilibrium dynamics (2) reads as

$$Rp_t = \sum_{h=1}^{2} n_{ht} p_{h,t+1}^e + y^*. \tag{5}$$

Fractions

Fractions n_{ht} are updated according to past performance, conditioned upon the deviation of actual prices from the fundamental value. The evolutionary competition part of the updating rules closely follows Brock and Hommes (1997a,b, 1998, 1999). The additional

[4]Gaunersdorfer (2000a) studies the case of time varying (homogeneous) beliefs about conditional variances. She obtains similar bifurcation routes to complicated asset price fluctuations as in the case with constant beliefs. We therefore restrict here to this more simple case. Chiarella and He (2000) introduce heterogeneity in beliefs about variances.

conditioning upon deviations from the fundamental was introduced in GH (2000) similar to the approach taken for instance in the Santa Fe artificial stock market in Arthur et al. (1997) and LeBaron et al. (1999).

In a first, evolutionary, step fractions are determined as discrete choice probabilities

$$\hat{n}_{ht} = \exp[\beta U_{h,t-1}]/Z_t, \qquad Z_t = \sum_h \exp[\beta U_{h,t-1}], \tag{6}$$

where U_{ht} is some 'fitness function' or 'performance measure'.[5] Note that the fractions are independent of the fitness level. The parameter β is called the intensity of choice. It measures how sensitive traders are to differences in performance of trading strategies. For $\beta = 0$ fractions are fixed over time and are – in the case of only two different types – equal to 1/2. In the limit of $\beta \to \infty$ all traders choose immediately the predictor with the best performance in the recent past. Thus, for finite, positive β agents are boundedly rational in the sense that fractions of the predictors are ranked according to their fitness.

The fitness function U_{ht} is defined as utility derived from realized profits, that is, risk adjusted realized profits. A straightforward computation (for details see Gaunersdorfer (2000a,b) and GH (2000)) shows that this results in

$$U_{ht} = -\frac{1}{2a\sigma^2}(p_t - p^e_{ht})^2 + \eta U_{h,t-1}, \tag{7}$$

i.e., fitness is determined by minus squared prediction errors. The parameter $0 \leq \eta \leq 1$ represents 'memory strength'.

In the second step of the updating conditioning on deviations from the fundamental by the technical traders is modeled as

$$\begin{array}{rcll} n_{2t} & = & \hat{n}_{2t} \exp[-(p_{t-1} - p^*)^2/\alpha], & \alpha > 0 \\ n_{1t} & = & 1 - n_{2t}. & \end{array} \tag{8}$$

According to (8) the fraction of technical traders decreases more, as prices deviate further from their fundamental value p^*. This is motivated by the fact that technical traders are conditioning their charts upon price deviations from the fundamental.

Notice that fractions in period t depend on *observed* prices up to the end of period $t-1$ (beginning of period t), $p_{t-1}, p_{t-2}, \ldots$. See GH (2000) for a more detailed discussion of the definition of the fractions and other aspects of the model.

Dynamical system

Setting $\hat{U}_{ht} = U_{h,t-1}$, we obtain the following dynamical system,

$$p_t = \frac{1}{R}(p^e_{1,t+1} + n_{2t}(p^e_{2,t+1} - p^e_{1,t+1}) + y^*) \tag{9}$$

$$\hat{U}_{ht} = -\frac{1}{2a\sigma^2}(p_{t-1} - p^e_{h,t-1})^2 + \eta \hat{U}_{h,t-1}, \quad h = 1, 2. \tag{10}$$

[5] Gaunersdorfer (2000b) introduces costs in the performance measure of the fundamentalists.

Introducing new variables $p_i(t-1) = p_{t-i}$, $u_h(t-1) = \hat{U}_{h,t-1}$, (9)–(10) is written as a six dimensional system in $(p_1, p_2, p_3, p_4, u_1, u_2) =: \mathbf{p}$. In the following we denote this system by Φ, where

$$\mathbf{p}(t) = \Phi(\mathbf{p}(t-1)).$$

Also, when working in a neighborhood of p^*, the mathematics becomes more transparant if local coordinates $(x_1, \cdots, x_4, u_1, u_2) =: \mathbf{x}$ are introduced by

$$x_i(t) = p_i(t) - p^*.$$

The system then takes the form

$$\begin{aligned} \Phi(\mathbf{x}) \;=\; & \left[\frac{1}{R}\Big((1-n_2)vx_1 + n_2(x_1 + g(x_1 - x_2))\Big), x_1, x_2, x_3, \right. \\ & \left. -\frac{1}{2a\sigma^2}(x_1 - vx_3)^2 + \eta u_1, -\frac{1}{2a\sigma^2}(x_1 - x_3 - g(x_3 - x_4))^2 + \eta u_2\right], \end{aligned} \tag{11}$$

where n_2 is given by

$$n_2 = \mathrm{e}^{-x_1^2/\alpha}\frac{\mathrm{e}^{\beta u_2}}{\mathrm{e}^{\beta u_1} + \mathrm{e}^{\beta u_2}}.$$

3 Stability analysis of the fundamental steady state

This section gives a local analysis of the dynamics at the fundamental steady state. In the first part it is shown that $\mathbf{x}^* = 0$ is the only steady state of (11). In the following, this will be called the *fundamental steady state* or the *fundamental* for short. The remainder of this section analyzes the stability of this fundamental steady state. It is stable for g close to 0, and it loses its stability in two different ways: period doubling bifurcations occur for certain negative values of g, while Hopf bifurcations occur for some positive g.

Period doubling and Hopf bifurcations are codimension one bifurcations, that is, they occur generically when a single parameter is varied. In subsection 3.3 the Hopf bifurcation is investigated in more detail. By inspecting its *normal form* (which is a simple representation of the system by choosing appropriate coordinates around the equilibrium), we note that for parameters in a certain set, these bifurcations can be degenerate and a so-called *Chenciner* bifurcation is said to occur. The Chenciner bifurcation is a codimension two bifurcation, that is, it occurs generically when varying two parameters. Codimension two bifurcation points are important, because they serve as 'organizing centers' of the codimension one bifurcation curves in the complete bifurcation diagram. In particular, close to a Chenciner bifurcation point a 'volatility clustering region' occurs, that is, an open region in the parameter space where a stable steady state and a stable limit cycle coexist. A short discussion of the theory of the Chenciner bifurcation is given in subsection 3.3.

3.1 Uniqueness and stability of the steady state

Lemma 1
Let $\Phi(\mathbf{x})$ be given by (11). Let moreover $R > 1$, $0 \leq v \leq 1$ and $0 \leq \eta < 1$. Then $\mathbf{x}^* = 0$ is the unique steady state of Φ.

Proof
Let $\mathbf{x}^*$ be any steady state of Φ, that is, let $\mathbf{x}^*$ satisfy

$$\mathbf{x}^* = \Phi(\mathbf{x}^*). \tag{12}$$

Notice first that $\mathbf{x}^* = 0$ is indeed a steady state. From the second, third and fourth component of equation (12), it follows that $x_1 = x_2 = x_3 = x_4$. Setting $x_1 = x$, the first component then reads as

$$Rx = (1 - n_2)vx + n_2 x.$$

Assuming that $x \neq 0$, we may divide both sides of this equation by x. But then we have

$$R = (1 - n_2)v + n_2 \leq \max\{v, 1\} < R,$$

which is a contradiction, hence $x = 0$. Now the last two components of equation (12) yield

$$u_1 = \eta u_1, \qquad u_2 = \eta u_2.$$

Since $\eta \neq 1$,[6] the lemma follows. ∎

Stability
In order to determine the stability of the fixed point the characteristic polynomial of the Jacobian $D\Phi(0)$ at the steady state is computed. It is given by

$$p(\lambda) = \lambda^2(\eta - \lambda)^2 \left(\lambda^2 - \frac{1 + g + v}{2R}\lambda + \frac{g}{2R}\right). \tag{13}$$

Thus, the eigenvalues of the Jacobian are 0, η (both of multiplicity 2) and the roots λ_1, λ_2 of the quadratic polynomial in the last bracket. Note that these roots satisfy the relations

$$\lambda_1 + \lambda_2 = \frac{1 + g + v}{2R} \qquad \text{and} \qquad \lambda_1\lambda_2 = \frac{g}{2R}. \tag{14}$$

Also note that the eigenvalues 0 and η always lie inside the unit circle. Thus, the stability of the steady state is determined by the absolute values of λ_1 and λ_2.

[6] For $\eta = 1$ the dynamical system has a *double* eigenvalue 1 (see equation (13)) and hence is non-generic in a two parameter system. Though this is an interesting case, it is – because of additional mathematical difficulties – beyond the scope of this paper to analyze it.

3.2 Codimension one bifurcations

As parameters are varied, bifurcations, that is, qualitative changes of the dynamical behavior will arise. In particular, bifurcations changing the (local) stability of the steady state may occur. At such a bifurcation value, the steady state must be non-hyperbolic having (at least) one eigenvalue of $D\Phi(0)$ with absolute value one, that is, one of the eigenvalues is equal to 1, -1, or there is a pair of complex eigenvalues having modulus 1. We first discuss the *codimension one* bifurcations, which are those bifurcations that are expected to occur (generically) when only a single parameter is varied.

Eigenvalue equal to 1
Assume that one of the eigenvalues λ_j is equal to 1, say $\lambda_2 = 1$. Then it follows from (14) that

$$\lambda_1 = \frac{g}{2R} \qquad \text{and} \qquad 1 + \lambda_1 = \frac{1 + g + v}{2R}.$$

Eliminating λ_1 from these equations leads to the condition

$$1 + v = 2R.$$

However, since $v \leq 1 < R$, this condition can never be satisfied. Hence eigenvalues equal to 1 cannot occur.

Eigenvalue equal to -1
Under the assumption that $\lambda_2 = -1$, equations (14) lead to the relations

$$\lambda_1 = -\frac{g}{2R} \qquad \text{and} \qquad -1 + \lambda_1 = \frac{1 + g + v}{2R}.$$

Eliminating λ_1 leads to

$$2g + v = -1 - 2R.$$

For parameters satisfying this equation, a *period-doubling* (also called *flip*) bifurcation of the steady state is found (if a certain nondegeneracy condition is satisfied).

Two complex conjugate eigenvalues of modulus 1
The roots λ_1, λ_2 of the characteristic equation are complex conjugate and of modulus one if $\lambda_1\lambda_2 = 1$ and $|\lambda_1 + \lambda_2| < 2$. Using (14), this leads to the conditions

$$\frac{g}{2R} = 1 \qquad \text{and} \qquad \left|\frac{1 + g + v}{2R}\right| < 2.$$

Substituting the first condition into the second yields

$$\left|1 + \frac{1 + v}{2R}\right| < 2.$$

For $0 \leq v \leq 1$, this condition is always satisfied, since $R > 1$. Hence, for parameters satisfying the equation

$$g = 2R,$$

a *Hopf* (also called *Neimark-Sacker*) bifurcation occurs (again if certain nondegeneracy conditions are satisfied; see subsection 3.3 and the appendix).

Conclusion
Introduce the functions $g_{PD}(\beta, v, R)$ and $g_H(\beta, v, R)$ by

$$g_{PD}(\beta, v, R) = -\frac{1}{2}(v + 2R + 1) \quad \text{and} \quad g_H(\beta, v, R) = 2R. \tag{15}$$

The following lemma summarizes the above discussion.

Lemma 2
The steady state $\mathbf{x}^* = 0$ *is hyperbolic for* $g \neq g_{PD}$ *and* $g \neq g_H$ *(*g_{PD} *and* g_H *defined by* (15)*). It is asymptotically stable for* $g_{PD} < g < g_H$*, and unstable for* $g > g_H$ *and* $g < g_{PD}$*.*

For $g = g_{PD}$ *or* $g = g_H$*, the fundamental steady state fails to be hyperbolic. In the first case* $D\Phi(0)$ *has an eigenvalue* -1*, in second case two complex conjugate eigenvalues of absolute value* 1*.*

If moreover in these latter cases certain nondegeneracy conditions are satisfied, then for $g = g_{PD}$ *the system undergoes a* period doubling (flip) *bifurcation, and for* $g = g_H$ *a* Hopf (Neimark-Sacker) *bifurcation.*

3.3 Codimension two bifurcations

In lemma 2 we mentioned necessary nondegeneracy conditions for the occurrence of period-doubling or Hopf bifurcations. This subsection investigates the situation that these non-degeneracy conditions are violated.

In the following, attention is restricted to the case of no memory in the performance measure ($\eta = 0$), and, since it is the economically more relevant case, to $g > 0$, that is, to the case of the Hopf bifurcation.

In that case, we obtain *degenerate Hopf* or *Chenciner* bifurcations, originally analyzed by Chenciner (1985a, 1985b, 1988), see also Kuznetsov (1998a) for a textbook treatment. The Chenciner bifurcation is a codimension two bifurcation: it is a non-generic phenomenon when only one parameter is varied, but a generic phenomenon when two parameters are varied simultaneously. We discuss the Chenciner bifurcation in some detail, since it is particularly relevant for the phenomenon of volatility clustering in our adaptive belief system, because close to the bifurcation point, there exists an open region in parameter space where a stable steady state and a stable attracting invariant circle coexist.

Nondegeneracy of the Hopf bifurcation
In the previous section, a surface in the space of parameters has been found for which $D\Phi(0)$ has two complex conjugate eigenvalues λ, $\bar{\lambda}$ of absolute value 1, and four eigenvalues with absolute values less than one. In this case, a two-dimensional *center manifold* W^c can be found that is invariant under the map Φ and tangent to the eigenspace

spanned by the eigenvectors associated to the eigenvalues λ, $\bar{\lambda}$. The nondegeneracy of the Hopf bifurcation can be decided by restricting attention to this manifold (for general references on center manifolds and nondegeneracy of bifurcations, see, for example, Guckenheimer and Holmes (1986) and Kuznetsov (1998a)).

In the following, we briefly discuss general normal forms of Hopf and Chenciner bifurcations. The system (11) will serve as the prime example.

Normal form transformation

By a so-called *normal form transformation*, that is, by a sequence of appropriate coordinate transformations, the map Φ restricted to the center manifold can be brought into the following *normal form*,

$$\varphi_\tau(z, \bar{z}) = \lambda(\tau)z + c(\tau)|z|^2 z + \dots .$$

Here the dots denote terms of higher order in z. Complex variables z, $\bar{z}$ are used to describe points on the two-dimensional real center manifold W^c. They are chosen such that $z = 0$ corresponds to the steady state of the full system Φ. The multi-dimensional parameter τ takes values in some *parameter space* P, which is usually an open subset of $\mathbb{R}^s$. For our model, P is equal to[7]

$$P = \{(\beta, v, g, R) \,:\, \beta > 0,\ 0 \le v \le 1,\ R > 1\}\,.$$

The coefficients $\lambda(\tau)$ of the linear part and $c(\tau)$ of the cubic part depend smoothly on $\tau \in P$.

Bifurcation manifold

There is a smooth (codimension 1) submanifold $\mathcal{H}$ of P, such that if $\tau \in \mathcal{H}$, the necessary condition for a Hopf bifurcation is fulfilled. Writing $\lambda = \lambda_1 + i\lambda_2$, this condition reads as

$$|\lambda| = 1, \qquad \lambda_2 \neq 0.$$

The manifold $\mathcal{H}$ is called a *Hopf bifurcation manifold*. Note that for our system (11)

$$\mathcal{H} = \{(\beta, v, g, R) \in P \,:\, g = 2R\}.$$

Nondegeneracy

The bifurcation is *nondegenerate* if

$$\mathrm{Re}\,\lambda(\tau)\overline{c(\tau)} \neq 0 \quad \text{and} \quad \mathrm{grad}_\tau|\lambda| \neq 0, \quad \text{for } \tau \in \mathcal{H},$$

[7] Changing the values of parameters a and σ is equivalent to choosing a different value for β, see equations (6) and (7). Further, by changing to new coordinates $\mathbf{x} = \sqrt{\alpha}\,\tilde{\mathbf{x}}$, the iteration equation (11) changes to $\sqrt{\alpha}\,\tilde{\mathbf{x}}_{t+1} = \Phi\left(\sqrt{\alpha}\,\tilde{\mathbf{x}}_t\right)$ and it follows, by some algebra, that $\tilde{\mathbf{x}}_{t+1} = \Phi\left(\tilde{\mathbf{x}}_t\right)$, where the parameter β is replaced by $\tilde{\beta} = \alpha\beta$. Thus, attention may be reduced to the case $\alpha = 1$. Hence we can restrict the parameter space of our model to P as given above (see also the Appendix).

where grad_τ denotes the derivative with respect to τ. The sign of $\mathrm{Re}\,\lambda\overline{c}$ determines the type of Hopf bifurcation: if it is negative (positive), a stable (unstable) invariant circle branches off the stable (unstable) fixed point $z = 0$, which becomes unstable (stable) as τ is varied and crosses $\mathcal{H}$. The Hopf bifurcation is called supercritical (subcritical).

For our evolutionary adaptive learning model, the locus of $\mathrm{Re}\,\lambda\bar{c} = 0$ is sketched in figure 1.

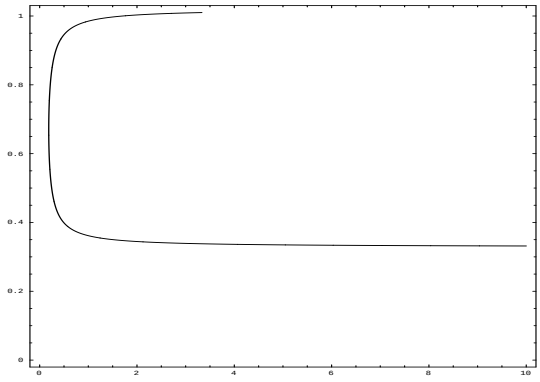

Figure 1: *Plot of the curve $\mathcal{C}$ of Chenciner bifurcation points lying within the Hopf bifurcation set $\mathcal{H} = \{g = 2R\}$ in the β-v-diagram, for $\beta \in [0, 10]$ and $v \in [0, 1]$.*

Chenciner bifurcation

If the nondegeneracy condition of the Hopf bifurcation is violated, then a *degenerate Hopf* or *Chenciner* bifurcation is said to occur. In the above notation, this happens for parameters $\tau \in \mathcal{H}$ such that

$$\mathrm{Re}\,\lambda(\tau)\overline{c(\tau)} = 0. \tag{16}$$

Condition (16) defines a codimension two manifold $\mathcal{C} \subset \mathcal{H}$ in the space of parameters. Again by performing normal form transformations, the restricted system can be brought into the following form, which is analogous to the normal form of the Hopf bifurcation with a fifth order term added,

$$\varphi_\tau(z, \bar{z}) = \lambda z + c|z|^2 z + d|z|^4 z + \dots .$$

Here $c = c(\tau) = 0$ if $\tau \in \mathcal{C}$, and both c and d depend smoothly on τ. This normal form is analyzed most easily in polar coordinates $z = re^{i\vartheta}$. Introducing parameters μ_1, μ_2 and ω by

$$\lambda = (1 + \mu_1)e^{i\omega}\,, \qquad \mathrm{Re}\,\lambda\bar{c} = \mu_2,$$

φ_τ takes the form

$$\varphi_\tau(r, \vartheta) = \left(r + \mu_1 r + \mu_2 r^3 + \gamma_1(\tau)r^5 + \dots, \vartheta + \omega + \gamma_2(\tau)r^2 + \dots\right). \tag{17}$$

All parameters are collected in a new multidimensional parameter, also called τ: $\tau = (\mu_1, \mu_2, \omega, \cdots)$. The nondegeneracy conditions for the Chenciner bifurcation are in these coordinates

$$\gamma_1(\tau) \neq 0 \neq \gamma_2(\tau).$$

Local bifurcation diagram

We discuss the structure of the local bifurcation diagram of the Chenciner bifurcation, illustrated in figure 2, using the normal form (17), where (for the time being) the higher order terms are set to zero. We discuss the case $\gamma_1(0) < 0$ and, without loss of generality, we assume that $\gamma_1(0) = -1$. See Kuznetsov (1995) for more information.

Note that any positive solution r_* to the equation

$$\mu_1 + \mu_2 r^2 - r^4 = 0,$$

or, equivalently, to

$$\left(r^2 - \frac{\mu_2}{2}\right)^2 = \frac{{\mu_2}^2}{4} + \mu_1, \tag{18}$$

corresponds to an invariant circle in phase space.

For $\mu_1 > 0$, equation (18) has exactly one positive solution. For $\mu_1 = 0$ equation (18) has a solution $r_* = 0$. Thus, $\mu_1 = 0$ is a line of Hopf bifurcations, whose type is determined by the sign of μ_2: for $\mu_2 < 0$, the Hopf bifurcation is supercritical, for $\mu_2 > 0$ it is subcritical.

The number of positive solutions for $\mu_1 < 0$ is determined by the sign of $\mu_2^2/4 + \mu_1$: there are two if it is positive, none if it is negative. Finally, for parameters on the curve

$$\mathcal{S} : \frac{{\mu_2}^2}{4} + \mu_1 = 0,$$

two positive roots of equation (18) coincide, making it a curve of saddle-node bifurcations of invariant circles.

For parameters not on either bifurcation curve, the invariant circles are *normally hyperbolic*. This implies that these circles are in a sense 'robust', they persist under small perturbations. A sketch of the bifurcation diagram is given in figure 2. Consider a point in parameter space $\{(\mu_1, \mu_2)\}$, with $\mu_1 < 0$ and $\mu_2 < 0$. For these parameter values the steady state is locally stable. Now fix μ_2 and increase μ_1. When crossing the μ_2-axis, for $\mu_1 = 0$, a supercritical Hopf bifurcation occurs, that is, a stable invariant circle is created and the steady state becomes unstable. Thus, in the region $\{\mu_1 > 0\}$ a stable limit cycle around an unstable steady state exists. Now fix a parameter value $\mu_2 > 0$ and decrease μ_1 from some positive value. When crossing the μ_2-axis again at $\mu_1 = 0$, a subcritical Hopf bifurcation occurs in which the steady state becomes stable, an unstable invariant circle emerges out of the steady state, and the stable invariant circle still exists. Decreasing μ_1 further, the unstable and stable circles approach each other and dissappear in a saddle-node bifurcation of invariant circles when μ_1 crosses the curve *SN*. Thus, in the region

between the positive μ_2-axes and the curve *SN* the system has two attractors, a stable steady state and an attracting (large) invariant circle, with an unstable invariant circle forming the boundary between these two attractors. We will call this region a *'volatility clustering region'*, since adding some noise to the system, the dynamics is characterized by an irregular switching between phases of small price fluctuations close to the steady state with small price changes and phases of large price fluctuations with large price changes along the limit cycle.

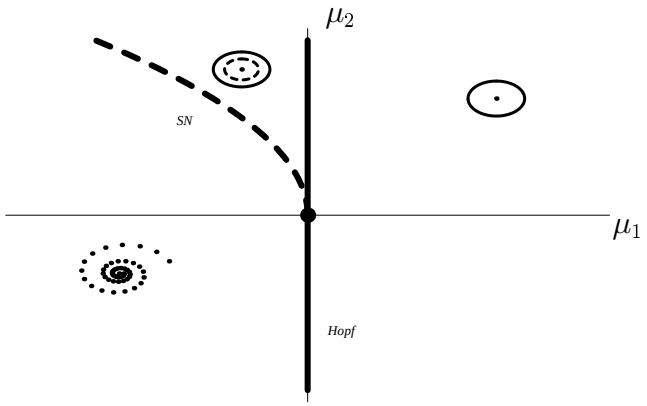

Figure 2: *Bifurcation diagram of the Chenciner bifurcation in the μ_1-μ_2-plane. The codimension two bifurcation point is in the origin of the coordinate system. The drawn lines are Hopf bifurcations, supercritical on one side of the Chenciner point ($\mu_2 < 0$), subcritical on the other ($\mu_2 > 0$). The dashed curve SN denotes a curve of saddle-node bifurcations of invariant circles. The 'volatility clustering region' is the region between the curve SN and the positive μ_2-axes, where a stable steady state and a stable limit circle coexist.*

Dynamics on the invariant circle

However, the situation is more complicated than sketched above, since the dynamics on the invariant circles may undergo bifurcations as well. For these dynamics there are two possibilities. The first possibility is that the dynamics on these circles consist of a sequence of attracting and repelling hyperbolic periodic points. This type of dynamics is called *resonating*, *phase locked* or *Morse-Smale*; for an example see figure 4 (middle plot). There is usually an open set of parameters for which the invariant circle has phase locked dynamics. The boundaries of this set are formed by saddle-node bifurcation curves of the attracting and repelling points on the invariant circle.[8] While the total set of parameters with phase locked dynamics is open and dense, its complement has positive measure. Parameters in the complement correspond to the case that the dynamics on the invariant circle are *quasi-periodic*; an example is shown in the left plot of figure 4. There is a large

[8]Pintus, Sands and de Vilder (2000) present an infinite horizon intertemporal equilibrium model exhibiting these types of local bifurcations after a Hopf bifurcation of the steady state, finally leading to strange attractors.

literature on quasi-periodic dynamics, to which the interested reader is referred (see Moser (1974), Herman (1979), Arnol'd (1983), Broer et al. (1990) and references there).

4 Global structure of the bifurcation diagram

In this section, the structure of the bifurcation diagram of the system is explored further. Above, the local bifurcations of the fixed point $\mathbf{x}^* = 0$ were determined analytically. Here, a sketch of the global bifurcation structure is attempted, at least at the onset of instability. The pictures in this section were generated using the numerical bifurcation packages AUTO97 (see Doedel et al. (1998)), CONTENT (Kuznetsov (1998b)) and DSTOOL (Back et al. (1992), Krauskopf and Osinga (1998)). We take $R = 1.01$ throughout this section.

4.1 Onset of instability

In the previous section it has been shown that in the case of $g > 0$, the fixed point $\mathbf{x}^* = 0$ is stable for small g, and it loses its stability in a Hopf bifurcation for $g = 2R$, as illustrated in figure 3. At $g = 2.09$ an invariant attracting circle, quasi-periodic (or periodic with high period), has appeared. For $g = 2.4$, the circle has developed into a strange attractor. The corresponding chaotic time series suggests some form of volatility clustering caused by intermittency.

However, attractors different from the fixed point can already exist before the Hopf bifurcation at $\mathbf{x}^* = 0$ takes place, as is shown in figure 4. Here attracting quasi-periodic circles exist already for $g = 1.60$. Since the origin is a stable fixed point up to $g = 2R = 2.02$, we conclude that here we have coexisting attractors. Note that coexisting attractors are a consequence of the occurrence of the Chenciner bifurcation discussed in section 3. Recall that it implies the existence of a codimension one manifold $\mathcal{S}$ in the space of parameters that carries a set of saddle-node bifurcation points of invariant circles.

This kind of saddle-node bifurcation is a 'global' phenomenon, in the sense that invariant circles are 'global' objects, and it typically occurs 'far away' from the fixed point. Except in small neighborhoods of Chenciner bifurcation points, no analytic information can be obtained about the location of the manifold $\mathcal{S}$.

A crude sketch of the location of $\mathcal{S}$ has been obtained as follows: for fixed values of β and v, plots of the phase space have been inspected visually for a range of g-values. The lowest value of g (to a precision of 0.01) for which an attractor other than $\mathbf{x}^* = 0$ existed, has been termed the (approximate) bifurcation value $g_*(\beta, v)$. See figure 5 for the graph $\mathcal{S}$ of g_*; in the second plot of figure 5, the set of Hopf bifurcations (plane $g = 2R$) is shown as well. Note that $\mathcal{S}$ can be seen as the set of *onset of instability* in the system. In the region bounded by $\mathcal{S}$ and $\mathcal{H}$ ('volatility clustering region'), the stable steady state and another attractor coexist. From the graph of $\mathcal{S}$ we conclude that, if the intensity of choice

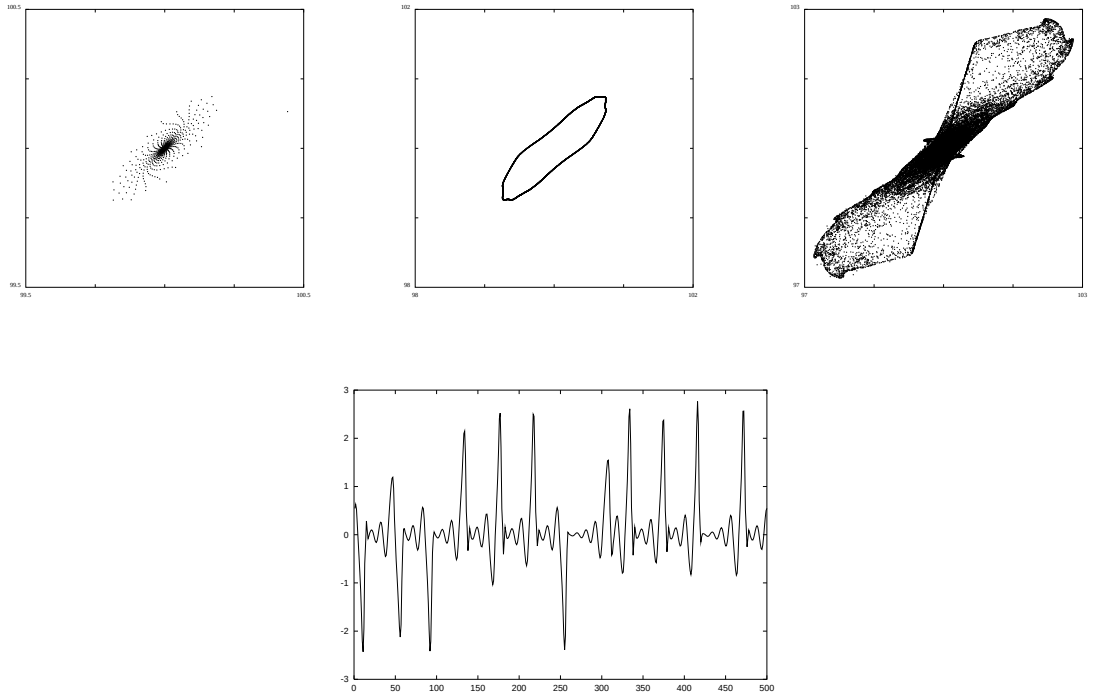

Figure 3: *Bottom panel: Projection of the attractors on the p_2-p_1-plane. Parameters are: $\beta = 4$, $v = 0.3$ and, from left to right, $g = 2$, $g = 2.09$ and $g = 2.4$. The fixed point is attracting in the leftmost picture: points spiraling towards it are shown. It undergoes a supercritical Hopf bifurcation at $g = 2.02$, has a quasiperiodic attractor for $g = 2.09$ and a strange attractor for $g = 2.4$ (shown in the middle and to the right, respectively). Bottom panel: Time series for the attractor of the top right plot showing intermittent chaos.*

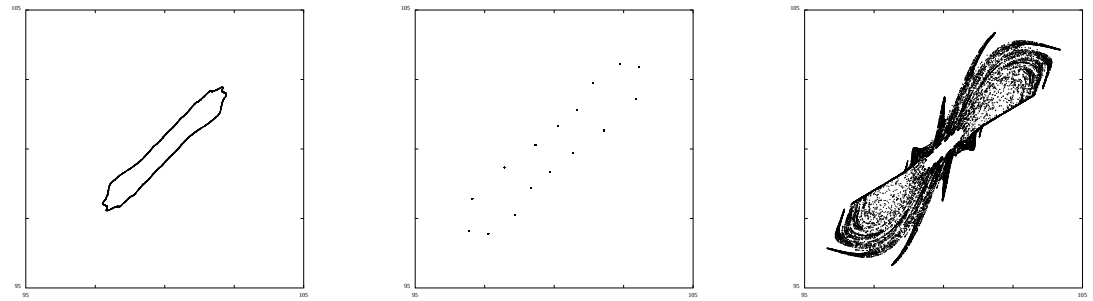

Figure 4: *Projections of a quasi-periodic, a periodic and a chaotic attractor on the p_2-p_1-plane. Not drawn is the stable fundamental steady state at $p^* = 100$. Parameters are: $\beta = 4$, $v = 0.6$ and, from left to right, $g = 1.60$, $g = 1.70$, and $g = 2.00$. These parameter values lie in the 'volatility clustering region' where two attractors coexist. The fixed point undergoes a subcritical Hopf bifurcation at $g = 2.02$. In the right figure the unstable invariant circle can be seen as the inner boundary of the strange attractor.*

β is high and v is in an intermediate range, say $0.4 \leq v \leq 0.8$, then a relatively small value of the trend parameter g already leads to coexistence of attractors and volatility clustering.

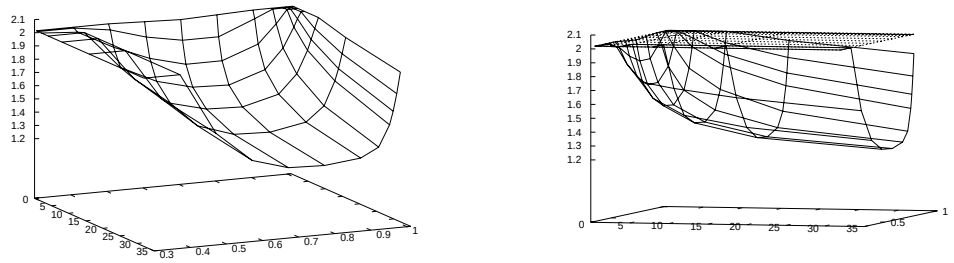

Figure 5: *The codimension one set $\mathcal{S}$ of saddle-node bifurcations of invariant circles at the onset of instability in (β, v, g)-space. In both pictures, the axes are oriented as usual, with the axis pointing to the top being the g-axis. In the right hand plot, the Hopf manifold $\mathcal{H}$ (the plane $g = 2R$) is plotted as well. Coexisting attractors occur in the region in between $\mathcal{S}$ and $\mathcal{H}$ ('volatility clustering region').*

4.2 Bifurcations past onset of instability

For values of g larger than $g_*(\beta, v)$, the structure of the bifurcation diagram becomes very rich, as testified by figures 6 and 7. Partly, this can be explained by the theory of the Chenciner bifurcation: there are many (probably countably many) curves of saddle-node bifurcations of periodic points on the invariant circles that are approximately tangent to $\mathcal{S}$.

Also homoclinic bifurcations of periodic points are predicted by the theory (Chenciner (1988)), and are found in the system, see figure 8. These imply in turn generically the existence of period-doubling cascades, horseshoes and infinitely many repelling or attracting periodic points and strange attractors (see Mora and Viana (1993), Palis and Takens (1993)).

Even for g in the 'unstable' region, the long run dynamics can become *regular*, periodic or quasi-periodic, and all the complicated structure (infinitely many periodic points and their stable and unstable manifolds) may be repelling and hence invisible. But typically, as parameters vary, for some parameter values this structure, or part of it, becomes stable and forms a strange attractor. This theme will be further explored in the next section.

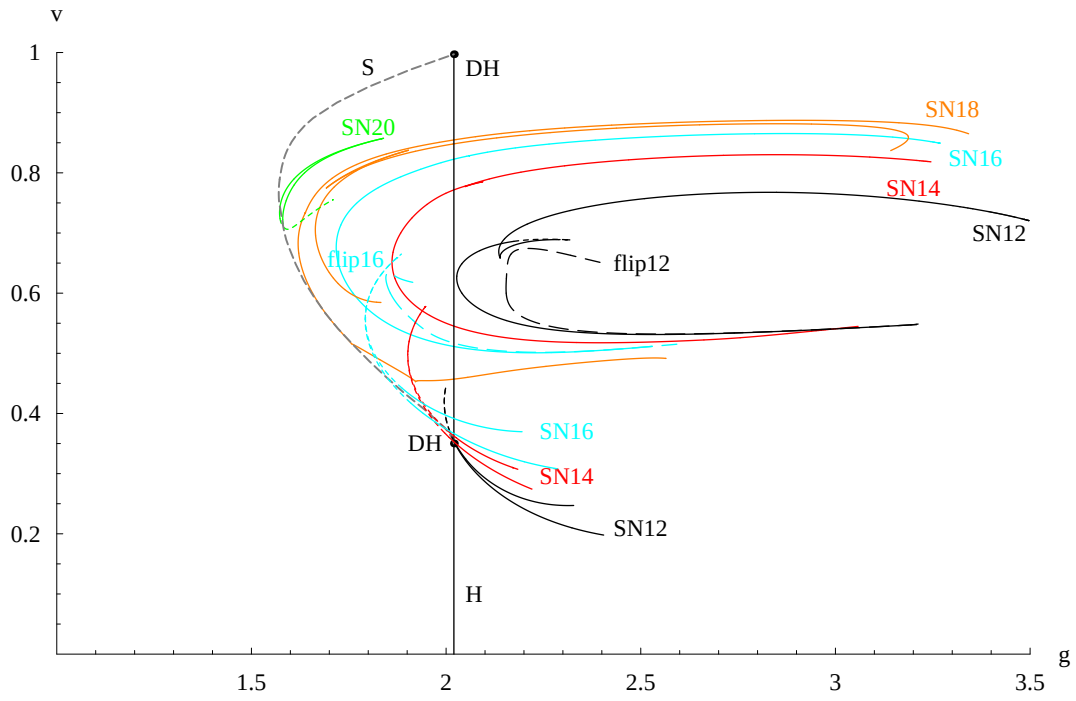

Figure 6: *Bifurcation diagram in the g-v-plane for* $\beta = 3$. *At the points* DH *a Chenciner bifurcation occurs. These points lie on the Hopf bifurcation line* H: $g = 2R$ *and are connected by a dashed line* S *corresponding to the saddle-node bifurcation curve of invariant circles. The area between* S *and* H *is the 'volatility clustering region'. SN*n *and flip*n *denote saddle-node and period-doubling (flip) curves respectively, of periodic points of period* n. *Many of the SN bifurcation curves accumulate on the curve* S, *the boundary of the onset of instability. Note that only a few of the (countably many) bifurcation curves are drawn here. Hopf and saddle-node bifurcations of periodic points with all hyperbolic eigenvalues lying in the unit circle are indicated by solid curves, flip curves by long dashes. Saddle-node curves of periodic points with one eigenvalue outside the unit circle are also short dashed.*

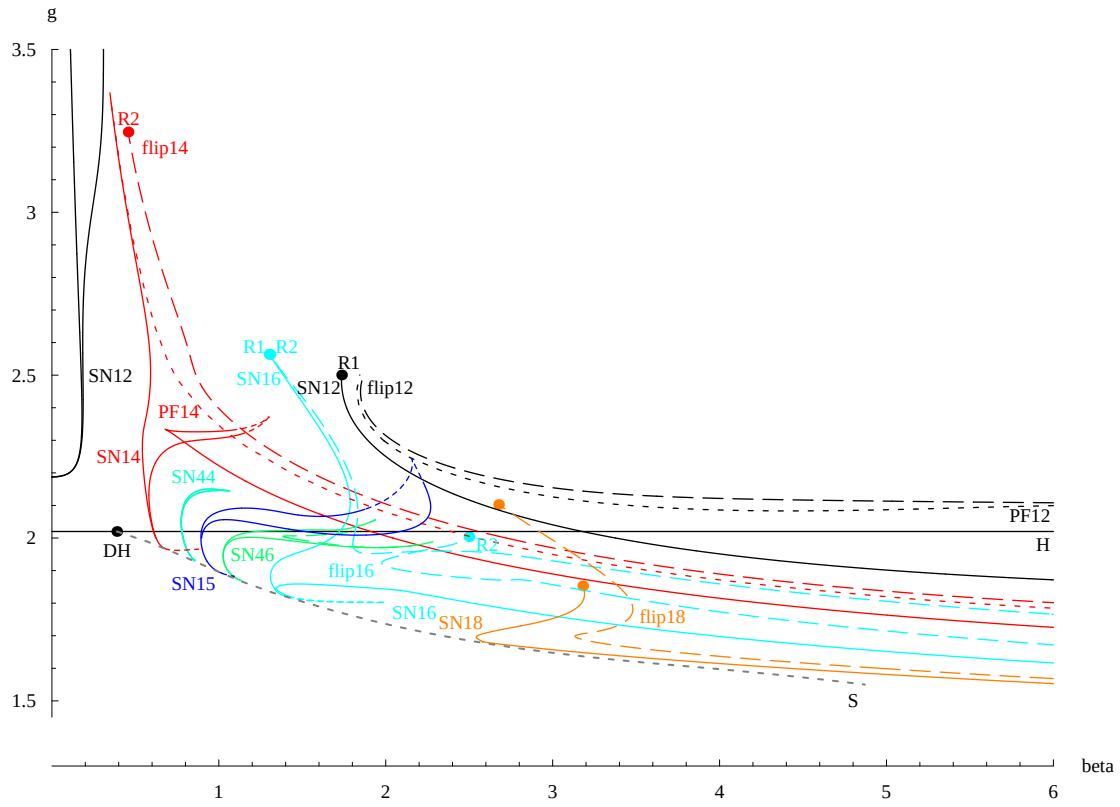

Figure 7: *Bifurcation diagram in the β-g-plane for $v = 0.6$. The point* DH *is a Chenciner bifurcation point, lying on the Hopf bifurcation line* H: $g = 2R$. *The lower dashed line* S *starting at the Chenciner bifurcation point corresponds to the saddle-node bifurcation curve of invariant circles. PF*n *denotes pitchfork bifurcations curves of points of period n, which are indicated by short dashes; further notation as in figure 6.*

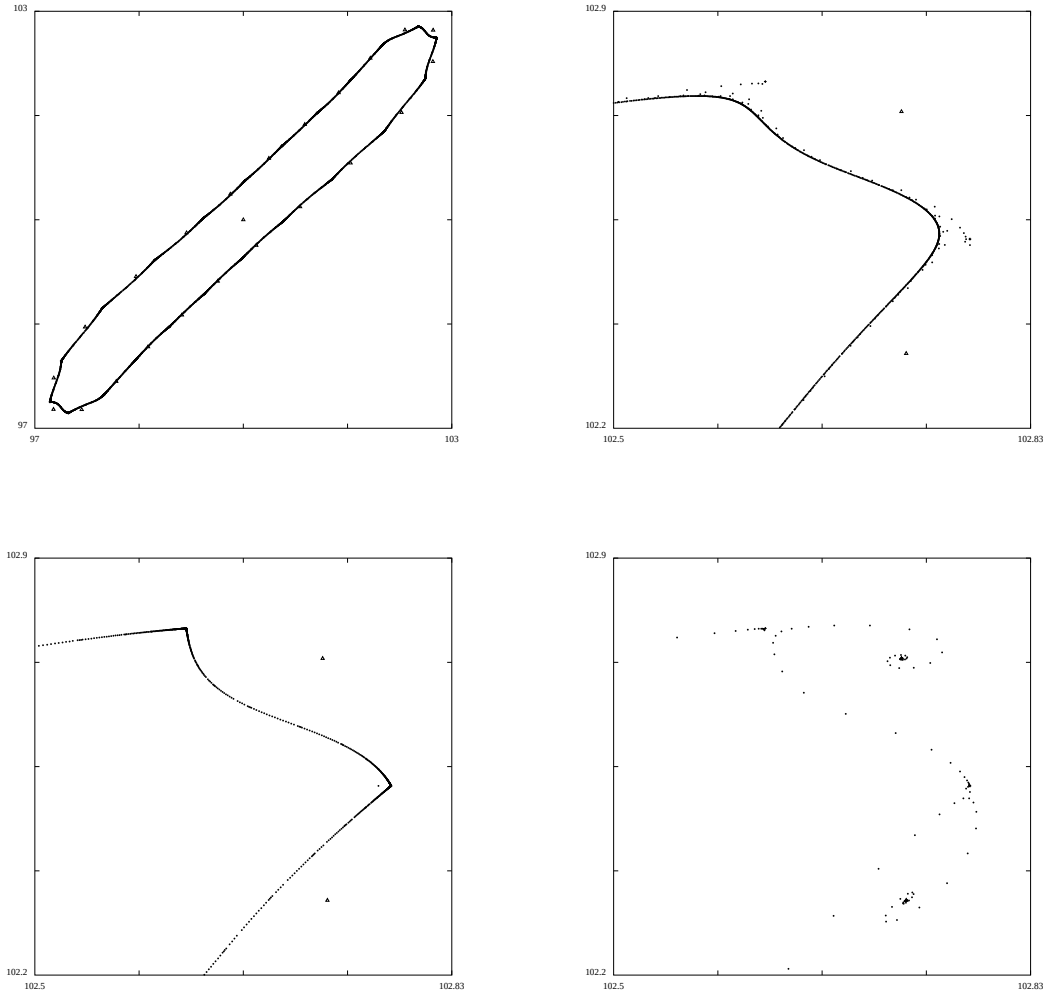

Figure 8: *Phase space plots in the p_2-p_1-plane for $\beta = 3$, $v = 0.8$ showing the disappearance of an invariant circle in a homoclinic bifurcation. Top left: $g = 1.57557$. Three coexisting attractors, the fundamental steady state, an attracting invariant circle, and a stable cycle of period 22 (marked as triangles) lying outside the invariant circle. The other three figures show details of phase plots for $g = 1.57553$ (top right), $g = 1.575576$ (bottom left) and $g = 1.57559$ (bottom right). Top right: points are attracted to an invariant circle, of which only a part is visible. Bottom left: the invariant circle (almost) connects consecutive saddle points. This situation is close to a so-called homoclinic bifurcation, hence the 'kinks' at the saddle points in the picture. Bottom right: after the homoclinic bifurcation value, points starting at the saddle converge to a period 22 sink. The invariant circle has disappeared*

5 Chaos

This section explores the occurrence of chaotic behavior in the model. First the location of chaotic dynamics in parameter space is determined by computing Lyapunov exponents. Then, mainly for the case that the parameter v is close to 1, the structure of the strange attractor is examined in more detail. We employ so-called one-dimensional *return plots*, defined for a suitable region in the phase space, to show the occurence of chaos. Such return plots can be used for all higher dimensional system which are close to a one-dimensional system in some suitable part of the phase space.

An intuitive argument why chaotic dynamics are likely to occur is the following. The dynamics of our model is characterized by the interaction of fundamentalists and technical traders extrapolating trends. As prices move away from the fundamental value the performance of fundamentalists is bad and price trends are reinforced by technical traders and prices will even move further away from the fundamental. However, as prices deviate too much technical traders become nervous, starting to believe that a price correction towards the fundamental is about to occur and their fraction decreases. This will cause prices to move towards the fundamental value. As prices approach the fundamental value trend traders will come into the market again and the story repeats.

Actually, this suggests reasons why the dynamics might be chaotic. A set of initial states of the system close to the fundamental will be stretched out during the phase when technical traders dominate. At the point where the fundamentalists start to become the dominating fraction in the market, the set will be folded back onto itself. The action of the fundamentalists transports this folded set back to the fundamental. See figure 11 below. It is precisely this stretching and folding which lies at the root of the occurrence of chaos in dynamical systems in general. Below we argue that this line of reasoning leads to a rather rigorous understanding of the source of at least some of the chaos in the present system. Technical trading causes stretching, whereas the conditioning of technical trading rules upon fundamentals causes folding in the adaptive belief system.

5.1 Regions of chaos

To get a global impression of the 'amount of chaos' to be expected in the system, *Lyapunov exponents* are computed for several values of the parameters.

Definition
If $\{\mathbf{x}_t\}_{t=0}^{\infty}$ is an orbit on an attractor, then the *first (or upper) Lyapunov exponent* λ is defined as:

$$\lambda = \lim_{t\to\infty} \frac{1}{n} \sum_{k=0}^{n-1} \log \|D\Phi(\mathbf{x}_t)\|.$$

The (upper) Lyapunov exponent measures the average rate of divergence (or convergence) of nearby trajectories. A system is commonly considered to be chaotic, if it has an attractor

such that orbits on the attractor have positive upper Lyapunov exponent.

For the present system, Lyapunov exponents have been computed for 10 different initial conditions, in order to account for the possibility of coexisting attractors. The largest value of the exponent obtained has been taken. These plots have been made both in the (β, g) (figure 9) and the (g, v) (figure 10) diagrams, given as a contour plot (right plots: region with positive Lyapunov exponents are indicated) and a 3D-plot (left plots: z-coordinate indicates magnitude of the Lyapunov exponent). For $g > 2R$ chaos seems to be the rule rather than the exception. But even for the stable region $g < 2R$, for parameters in the 'volatility clustering region' a coexisting chaotic attractor may exist (cf. also figure 4).

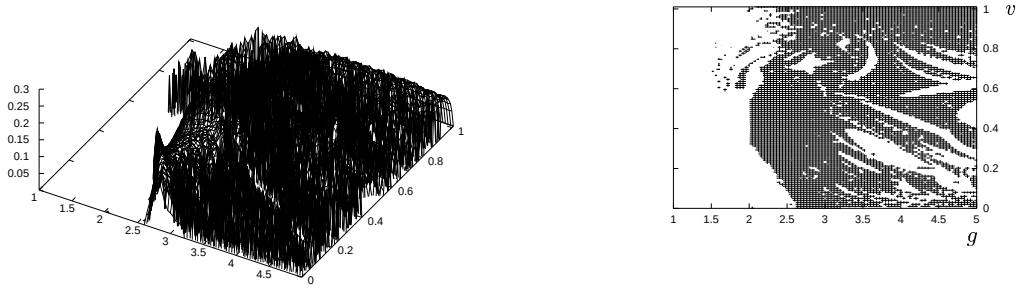

Figure 9: *Lyapunov exponents for $g \in [1, 5]$, $v \in [0, 1]$, $\beta = 3$: on the left, the magnitude of the upper Lyapunov exponent is plotted along the z-axis. In the right picture, for points in the grey area, upper Lyapunov exponents are positive – for those parameters, there is a chaotic attractor (compare the bifurcation diagram in figure 6).*

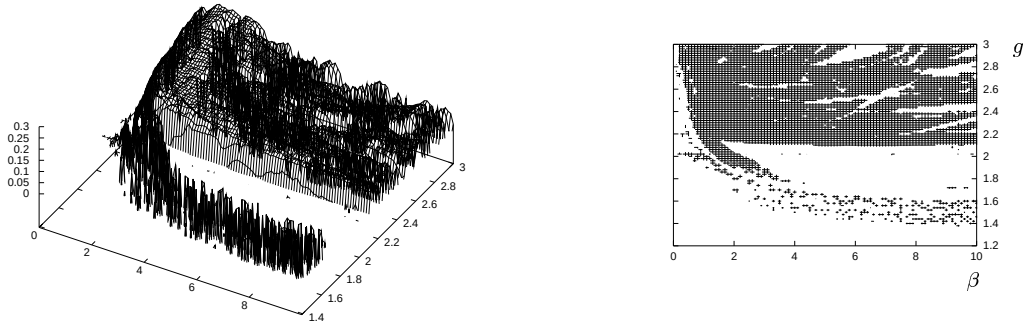

Figure 10: *Lyapunov exponents for $\beta \in [0, 10]$, $g \in [1.2, 3]$ (compare the bifurcation diagram in figure 7). Legend as in figure 9.*

5.2 Structure of the dynamics

First, some qualitative remarks are made. Note that if the fundamentalists dominate the market ($n_1 \approx 1$, $n_2 \approx 0$), they determine the new price, which will be close to

$$x_1 = \frac{v}{R} x_2. \tag{19}$$

If the domination extends over several periods, the corresponding phase points in the x_2-x_1 diagram will lie close to the line ℓ given by

$$\ell : \quad x_1 = \frac{v}{R} x_2.$$

However, if the trend chasers dominate, then the new price will be close to

$$x_1 = \frac{1+g}{R} x_2 - \frac{g}{R} x_3. \tag{20}$$

This rule corresponds to a one-parameter family of curves close to the family of straight lines[9]

$$m_b : \quad x_1 = g x_2 + b, \tag{21}$$

where $b \in \mathbb{R}$ is a parameter that depends on the initial values of x_1 and x_2.

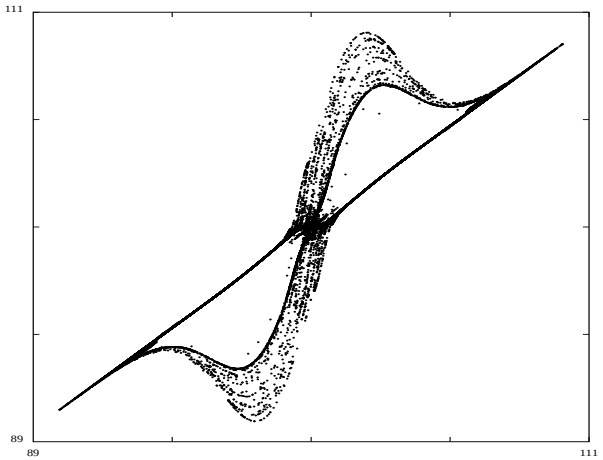

Figure 11: *A strange attractor in phase space, projected onto the p_2-p_1-plane, for parameters $(\beta, g, v, R, \alpha) = (10, 5, 0.95, 1.01, 10)$. On the attractor, $5 \cdot 10^4$ points are plotted. Note the pronounced line ℓ, which is approximately equal to $x_1 = 0.94 x_2$, as well as a family of curves with slope approximately equal to 5 close to the origin.*

Example

We discuss the global features of the dynamics with parameters equal to

$$(\beta, g, v, R) = (10, 5, 0.95, 1.01),$$

and with $\alpha = 10$. Note that these parameter values are not intended to reflect an economically relevant situation; in particular, the value $g = 5$ is much too high to be realistic.

[9] For $R = 1$, (20) implies that the dynamics dominated by trend followers lies on a straight line (21) close to the origin. This can be seen by substituting (21) repeatedly into (20) and solving for coefficients. For R close to 1, the family of lines (21) is replaced by a family of curves approximating these straight lines at the origin.

However, this situation serves very well to illustrate the dynamics of the model. See figure 11 for a plot of $4 \cdot 10^4$ iterates on the attractor.

Note that both the line ℓ and the family of lines m_b are clearly visible, at least close to the fundamental. They turn into curves away from the fundamental, due to the influence of the term $\mathrm{e}^{-x_1^2/\alpha}$. Notice that close to the origin, several trajectories depart from ℓ. Points which where close while on ℓ are there drawn apart in the unstable directions of the fixed point.

Return plots

To obtain more information on the dynamics, return plots have been made in figure 12. They use the fact that in the phase where the fundamentalists dominate, all points travel close to the one-dimensional line ℓ, and there they are effectively characterized by a single coordinate, for instance x_1.[10] A point $\mathbf{x}^*$ is taken on the attractor and near the line ℓ. Its image under iteration is denoted $\mathbf{x}_* = \Phi(\mathbf{x}^*)$. A *fundamental set* F is introduced by

$$F = (x_{*1}, x_1^*]\,.$$

Now a relation $R \subset F \times F$ is defined as follows. Let $\mathbf{x}$ be such that its first coordinate x_1 is in F. Let $\mathbf{y}$ be the first iterate of $\mathbf{x}$ under Φ such that $y_1 \in F$ and $n_2(\mathbf{y}) \leq c$. This last condition is needed in order to insure that the point $\mathbf{y}$ will again be close to ℓ, that is, it will be a point of the branch dominated by fundamentalists. Typically $c \leq 0.4$ was taken. Then the relation R is given by

$$(x_1, y_1) \in R.$$

This relation can be plotted by forward iteration of a single point (for instance, for parameters where by inspection of plots of the phase space chaos is expected). This has been done in figures 12–13 below. In case of figure 12, graphical evidence suggests that there the relation R is actually described by a function φ,

$$R = \{(x_1, y_1) \,:\, y_1 = \varphi(x_1)\}\,,$$

and that, consequently, the system is equivalent to a one-dimensional dynamical system. Since the endpoints of F can be identified, φ can be thought of as a circle map. Note first that the maps in figure 12 have on a large set large derivatives. As remarked in the caption of figure 12, as β increases, a critical value of the map increases steadily (the 'hump' in the right hand side of the picture). If the corresponding critical point is nondegenerate, the theory of circle embeddings (Newhouse et al. (1983)) can be brought to bear on the system, insuring the existence of a nondegenerate homoclinic tangency. Then results of Jakobson (1981) and Mora and Viana (1993) insure the existence of strange attractors for a set of parameters of positive measure.[11]

[10] Hommes (1992) contains an example of a two-dimensional piecewise linear model analyzed by a one-dimensional return map of a suitable line segment in the phase space.

[11] If the critical point is degenerate, at least arbitrarily close to the system, there is another system with this property.

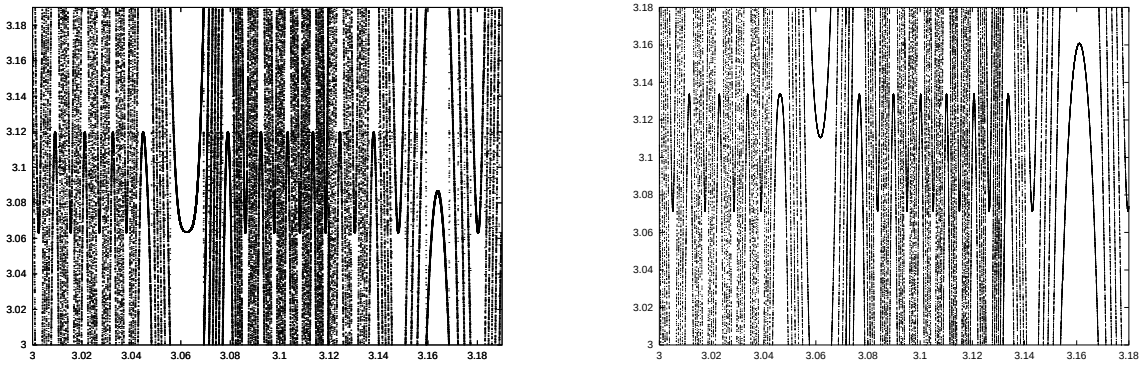

Figure 12: *Return map to a fundamental domain, for* $\beta = 8$ *(left) and* $\beta = 10$ *(right), respectively. The other parameters are fixed at* $(g, v) = (5, 0.95)$. *Notice the parabolic shape on the right hand side of the pictures, whose critical value increases as* β *increases. This suggests strongly the presence of the familiar 'quadratic family chaos' in the model. This plot illustrates the stretching and folding described at the beginning of section 5: the monotonic branches (the steep parts) of the graphs correspond to the stretching, the humps correspond to the folding.*

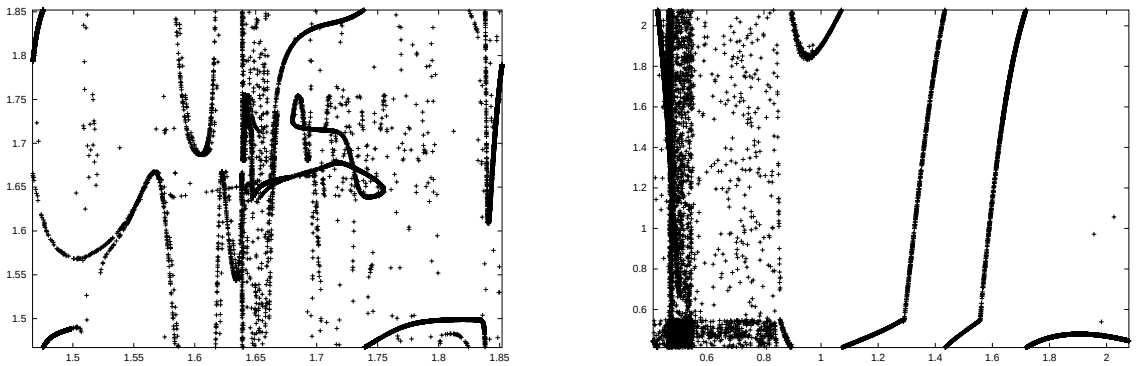

Figure 13: *Examples where the relation* R *cannot be described by a function. On the left side* $(\beta, g, v) = (9, 3.2, 0.8)$*; note that the set of points cannot be parametrized by a graph, yet there is a lot of one-dimensional structure in the picture. On the right* $(\beta, g, v) = (6, 3, 0.2)$*; in some parts the description with a graph is very good, while it breaks down in others.*

This one-dimensional description of the system fails notably in the cases of figure 13, where the dynamics are intrinsically higher dimensional. However, even in those cases, the stretching and folding that generate chaos are apparent.

6 A normal form with noise

GH (2000) investigated time series properties of the adaptive belief system studied here, buffeted with dynamic noise, and compared the autocorrelation structures of returns and squared returns to those observed in 40 years of daily S&P 500 data. The matching of the autocorrelation patterns has essentially been done by extensive trial and error simulation of the adaptive belief system with noise and visual inspection. This section presents a model of the adaptive belief system with noise: a simple one-dimensional "normal form" with dynamic noise, motivated by our bifurcation analysis of the GH-model. This simple nonlinear stochastic model generates strong volatility clustering with slowly decaying positive autocorrelations of squared returns in the presence of rapidly vanishing autocorrelations of returns, similar to those observed in real financial data.

Universality of bifurcation normal forms
Bifurcations are qualitative changes of the geometry of orbits in phase space, and in that sense universal to all dynamical systems. Those bifurcations that are of low codimension can be brought, by an appropriate choice of coordinates (normal form transformation), into a particularly simple form, characterized by only a few parameters. A normal form is in fact a reduction of the map at the bifurcation value to the minimum number of nonlinear (polynomial) terms and the minimum number of parameters. There is a large literature on unit root properties of economic time series. This suggests that in order to get insight into the mathematical mechanism generating statistical properties such as volatility clustering, it makes sense to investigate time series obtained from the normal form of a bifurcation, buffeted with noise. It is to be expected that the full system displays the same statistical properties, especially when the parameter values are close to the particular bifurcation point. Turning the argument around, knowledge of the time series behavior of a normal form buffeted with noise gives indications to where to look, and what to look for in the full system, if certain statistical properties are to be emulated.

Recall that the normal form of the Chenciner bifurcation in (17) reads as

$$\varphi_\tau(r,\vartheta) = \left(r + \mu_1 r + \mu_2 r^3 - \gamma_1(\tau) r^5 + \ldots, \vartheta + \omega + \gamma_2(\tau) r^2 + \ldots\right). \tag{22}$$

Recall also from subsection 3.3 that the (complex) eigenvalue of the linearized system is $\lambda = (1+\mu_1)e^{i\omega}$, where μ_1 determines the (in)stability of the steady state and ω determines the rotation around the steady state. In numerical simulations of the Chenciner normal form buffeted with noise volatility clustering occurs, but at the same time significant autocorrelations of returns, defined as relative changes, also may arise, especially when the rotation parameter ω is *not* close to zero. For ω close to zero, the ϑ component in (22)

only changes slowly and moreover does not affect the r-component up to order 5. If the ϑ-component is dropped, and r is taken to range over $\mathbb{R}$ instead of $\mathbb{R}_+$, we get the normal form of the degenerate pitchfork bifurcation.

System specification

The normal form of the degenerate pitchfork reads as

$$\varphi_\mu(r) = r + \mu_1 r + \mu_2 r^3 - \gamma_1 r^5 + \dots \ .$$

To investigate the dynamics of this normal form buffeted with Gaussian noise, the 'dots' have to be specified. This has been done in such a way that the map φ_μ is a diffeomorphism, that is, a smooth map with a smooth inverse, bounded at plus and minus infinity. The following diffeomorphism is taken

$$\tilde{\varphi}_\mu(r) = \frac{r + \mu_1 r + \mu_2 r^3 - \gamma_1 r^4 \arctan 10r + \gamma_2 r^{10} \arctan 20r}{1 + \gamma_3 r^{10}} + \varepsilon.$$

The graph of the map φ_μ is shown in figure 14. Note that the arctan terms ensure that the map is bounded and that the dynamics remain in a (small) neighborhood of the origin. Notice also that in a neighbourhood of the origin up to fifth order terms in r $\tilde{\varphi}_\mu \approx \varphi_\mu$. The map has five fixed points: a stable fixed point at the origin, surrounded by two unstable fixed points, one positive and one negative, and two additional stable fixed points, one positive and negative, outside the interval bounded by the unstable fixed points. Recall that, as the rotation parameter ω goes to zero, the Chenciner bifurcation normal form (22) approaches the degenerate pitchfork bifucation normal form.[12] Therefore, since the parameters μ_1 and μ_2 have been chosen in the volatility clustering region, the unstable fixed points of the degenerate pitchfork may be thought of as corresponding to the inner unstable invariant circle of the Chenciner bifucation with small rotation around the stable steady state, and the stable fixed points of the pitchfork relate to the outer stable invariant circle in the same way.

We generated time series from the normal form model buffeted with noise, that is,

$$r_{t+1} = \tilde{\varphi}_\mu(r_t) + \varepsilon_t,$$

where ε_t is a white noise term, that is, identically and indepentently drawn from a $\mathcal{N}(0, \sigma_\varepsilon)$ distribution. The variable r_t should be thought of as a price deviation from a fundamental price p^*. The results of the simulation are given in figure 15. The top panel shows the time series of the 'prices' $p_t = r_t + p^*$ and the corresponding 'returns'

$$\frac{p_{t+1} - p_t}{p_t} = \frac{r_{t+1} - r_t}{r_t + p^*}.$$

The 'price' series is higly persistent, whereas the 'returns' series is higly unpredictable and clearly shows volatility clustering. The autocorrelations of squared returns are significantly positive and decay slowly.

[12] Note however, that the Chenciner normal form ceases to be valid in this case since the normal form transformation is singular for $\omega = 0$.

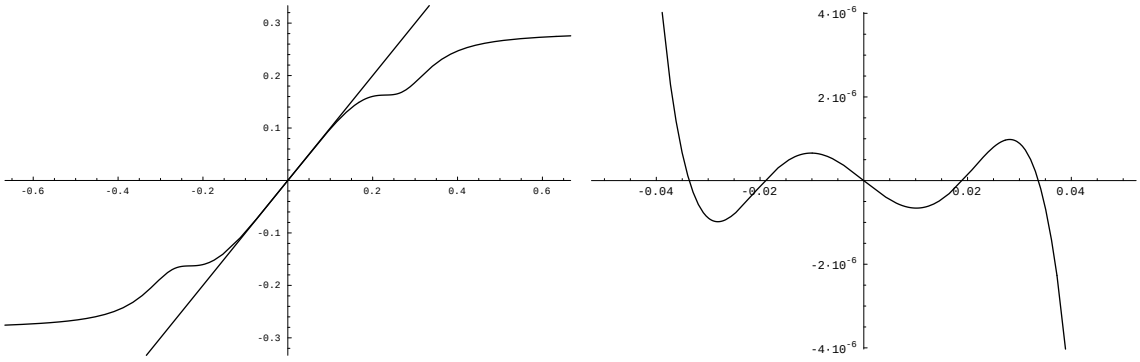

Figure 14: *Graph of the degenerate pitchfork normal form map* $\tilde{\varphi}_\mu$ *for* $\mu_1 = -10^{-4}$, $\mu_2 = 0.368$ *and higher order term parameters* $\gamma_1 = 25.6$, $\gamma_2 = 58254.2$ *and* $\gamma_1 = 314572.8$ *(left) and graph of the difference* $\tilde{\varphi}_\mu(r) - r$. *The map has five fixed points, one stable at* 0, *two unstable fixed points close to* 0 *and two stable fixed points further away from* 0. *Notice also that there is an interval around* 0 *where the graph of* $\tilde{\varphi}_\mu$ *is close to the diagonal.*

It is remarkable that our example bears some resemblance to an example of a simple first order nonlinear autoregressive time series model, exhibiting slowly decaying autocorrelation functions and long memory effects as in Granger and Teräsvirta (1999). The reader is urged to compare figure 1 in Granger and Teräsvirta (1999) to our 'price' series in figure 15 (top left). Granger and Teräsvirta (1999) have two stable states, one high and one low, and if the probability of switching between the two states is low, the system has slowly decaying autocorrelations and long memory. Our system has three stable states, a high state, a low state and the middle fundamental state. The 'price' series in figure 15 (top left) shows irregular switching between these three stable states and, as a consequence, the corresponding returns series (top right) shows irregular switching between phases of high and low volatility.

Our simulations show that normal form models buffeted with noise can reproduce volatility clustering and long memory effects. The normal form (22) yields the best results for the rotation parameter ω close to zero, implying that the two complex eigenvalues are close to an eigenvalue $+1$. For the adaptive belief system a double eigenvalue $+1$ occurs when $g = 2R$ and $v = 2R - 1$. In particular, for $v = 2R - 1$ the adaptive belief system has always an eigenvalue $+1$. Since R is close to 1, this implies that for $v = 1$ the system is close to having a unit root, and this may explain why GH (2000) get the best statistical properties and strong volatility clustering in the adaptive belief system with noise for $v = 1$.

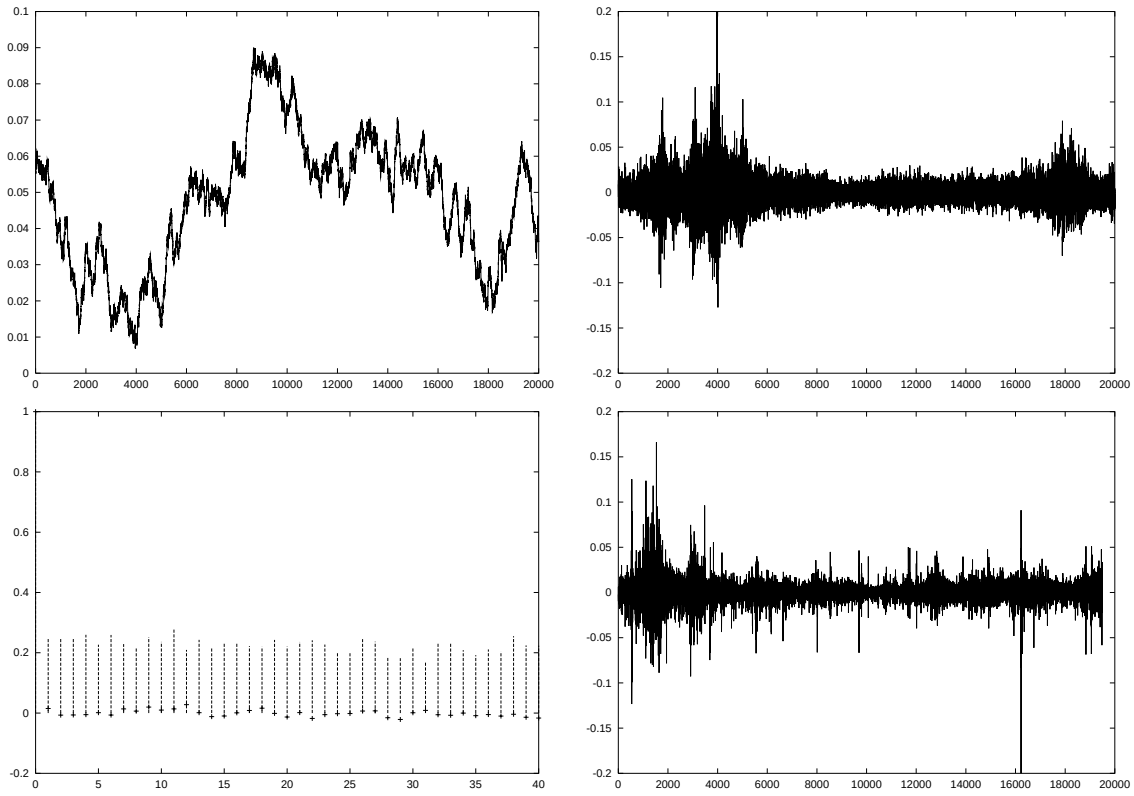

Figure 15: *The normal form system of the degenerate pitchfork bifurcation for the parameters* $\mu_1 = -10^{-4}$, $\mu_2 = 0.368$, $\gamma_1 = 25.6$, $\gamma_2 = 58254.2$ *and* $\gamma_1 = 314572.8$, *with Gaussian noise* ($\sigma_\varepsilon = 0.002$) *added. The fundamental price level was chosen to be* $p^* = 0.055$. *Top left, time series of the prices. Top right, returns of this time series are shown. Bottom left the first* 40 *autocorrelations of the returns (crosses) and of the squared returns (drawn bars); bottom right, for comparison, the time series of the returns of daily S&P 500 index from the last 80 years.*

7 Conclusions

In this paper we present a simple, nonlinear structural model for volatility clustering, based on the concept of evolutionary adaptive belief systems introduced by BH (1997a). Volatility clustering arises endogenously due to the interaction between fundamentalists and technical analysts driven by adaptive learning. Two mechanisms are proposed as an explanation: intermittency and coexistence of attractors. Chaos arises from the combination of stretching due to trend extrapolation by chartists and folding due to conditioning of the forecasting rules upon market fundamentals. Coexistence of attractors arises due to a codimension two Chenciner bifurcation. Close to the Chenciner bifurcation there is a "volatility clustering region", that is, an open set in parameter space where a stable steady state and a stable invariant circle coexist. Both mechanisms proposed are generic phenomena and thus may serve as explanations of volatility clustering in more complicated computational multi-agent systems.

We have also proposed to model the adaptive belief system with noise by a one-dimensional normal form model buffeted with dynamic noise. This simple normal form model is able to generate unpredictable returns and strong volatility clustering with slowly decaying autocorrelations in squared returns similar to those observed e.g. in the S&P 500 data.

Two extensions seem worthwhile investigating in future work. Normal form models from bifurcation theory buffeted with noise may generate some of the stylized facts in financial data. Normal forms originate from bifurcation theory and are in fact simple unit root models, with a minimum number of (polynomial) nonlinear terms and parameters, corresponding to that type of bifurcation. We use the so-called degenerate pitchfork bifurcation normal form (with noise) because it is in some sense close to the Chenciner bifurcation that occurs in our adaptive belief system. A systematic investigation of the statistical properties of noisy normal forms of bifurcations of low codimension would be useful.

The adaptive belief system has been formulated around a benchmark fundamental. In this paper we have focussed exclusively on the case of a constant fundamental, derived from an underlying IID dividend process. A second natural extension seems to be to investigate the evolutionary adaptive system in the case of more realistic dividend and time varying fundamental processes, for example a geometric random walk, and see whether such non-stationary models match the data more closely. We leave all this for future work.

A Normal form computations

The purpose of this appendix is to give a normal form analysis of the Hopf bifurcations at the origin in the GH-model and, in particular, compute the curve of codimension two Chenciner bifurcation points as shown in figure 1. This section recalls briefly that part of normal form theory that is relevant for the analysis of a Hopf bifurcation. For a fairly complete treatment of bifurcation theory see, for example, Guckenheimer and Holmes (1986) and Kuznetsov (1998).

Definitions

Note that in everything that follows, *deviations* $x_t = x(t)$ are used instead of prices $p_t = p(t)$. They are introduced in terms of the fundamental price p^*:

$$x(t) = p(t) - p^*.$$

Note that the 'fundamental' fixed point p^* corresponds with $x = 0$. This convenience is the main reason for the change of variables.

Consider a family of maps $\varphi_\mu : \mathbb{R}^m \to \mathbb{R}^m$ such that $\varphi_\mu(0) = 0$; that is, 0 is a fixed point of all maps of the family. Here μ is a multi-dimensional parameter, taking values in an open subset P in $\mathbb{R}^s$; P is called the *parameter space*. Note that the dependence on μ will not always be indicated, in order not to overburden the notation.

Given an initial value x_0, an *orbit* $\{x(t)\}$ of the system is defined by:

$$x(t) = \varphi_\mu(x(t-1)) = \varphi_\mu^t(x_0), \qquad \text{for } t > 0.$$

Notation

For nonnegative functions $f(x)$, the 'big-O' notation will be used for remainder terms $R(x)$ which are of the form $R = R_1 + R_2 + \cdots + R_n$, such that:

$$\lim_{|x|\to 0} \frac{|R_j(x)|}{f_j(x)} = 0,$$

for nonnegative functions $f_j(x)$. This will be denoted by:

$$\mathrm{O}\left(f_1(x), \cdots, f_n(x)\right).$$

Linearization

Let A denote $D\varphi_\mu(0) = \mathrm{d}\varphi_\mu/\,\mathrm{d}x(0)$, the Jacobian matrix of φ_μ at 0. Then φ_μ can be written as:

$$\varphi_\mu(x) = Ax + N(x),$$

where $N(x) = \mathrm{O}(|x|^2)$.

If an eigenvalue of A has absolute values different from 1, it is called a *hyperbolic* eigenvalue. If all eigenvalues of A are hyperbolic, the point 0 is called a *hyperbolic* fixed point. However, if for some $\mu = \mu_0$, there is one ore more eigenvalue λ such that $|\lambda| = 1$, the fixed point 0 is called *nonhyperbolic*, and the family φ_μ is said to *bifurcate* at $\mu = \mu_0$.

This note is interested in the case that there are precisely two nonhyperbolic eigenvalues $\lambda_\pm$, which satisfy the following *nonresonance* condition:

$$\lambda_\pm \notin \left\{ \mathrm{e}^{2\pi i \frac{p}{q}} \,:\, p, q = 1, \cdots, 6 \right\}. \tag{23}$$

Centre space and centre manifold

The eigenvectors associated to these eigenvalues span a two-dimensional linear space, the *linear centre space* E^c. The remaining eigenvectors span the so-called *hyperbolic* space E^h. Note that the sum of these two spaces is equal to $\mathbb{R}^n$:

$$E^c + E^h = \mathbb{R}^n.$$

The map φ can be written as $\varphi = (\zeta, \eta)$, where for $x_c \in E^c$ and $x_h \in E^h$:

$$\zeta(x_c, x_h) \in E^c, \qquad \eta(x_c, x_h) \in E^h.$$

At a bifurcation, the 'interesting' dynamics occurs on an invariant manifold W^c which is tangent to the linear space E^c at 0, the so-called *centre manifold* (see Guckenheimer and Holmes (1986) for more information). Locally around 0, this manifold can be described as the graph of a function $w(x_c)$:

$$w : E^c \to E^h, \qquad w(x_c) = \mathrm{O}(|x|^2).$$

The 'interesting' dynamics ψ are precisely given by the map φ restricted to the centre manifold W^c:

$$\psi(x_c) = \zeta\left(x_c, w(x_c)\right).$$

Note that ψ maps E^c to itself: the dynamics have been 'pulled' to the linear centre space, that is to the plane $\mathbb{R}^2$ in the present case of two nonhyperbolic eigenvalues.

Normal form

Since the nonhyperbolic eigenvalues $\lambda_\pm$ are complex, it turns out to be convenient to introduce complex coordinates $(z, \bar{z})$ in the plane. In these coordinates, the map ψ can be written as:

$$\psi(z, \bar{z}) = \lambda z + f(z, \bar{z}),$$

where $f = \mathrm{O}(|z|^2)$. An orbit $\{(z(t), \bar{z}(t))\}$ is now given by:

$$z(t) = \psi(z(t-1), \bar{z}(t-1)), \qquad \bar{z}(t) = \overline{\psi(z(t-1), \bar{z}(t-1))}.$$

The *normal form procedure* performs a series of coordinate changes:

$$u = H_j(z, \bar{z}) = z + \sum_{m+n=j} h_{mn} z^m \bar{z}^n,$$

where m, n take only nonnegative integer values, such that in the new coordinates the form of ψ is as 'simple' as possible. In the present case, and under the present nonresonance condition (23), ψ can be transformed into the following form:

$$\tilde{\psi}(z, \bar{z}) = \lambda z + a_1 z|z|^2 + a_2 z|z|^4 + \mathrm{O}(|z|^6).$$

If:

$$\mathrm{Re}\, \bar{\lambda} a_1 \neq 0, \tag{24}$$

then the point 0 is said to undergo a *Hopf bifurcation* at $\mu = \mu_0$. However, if condition (24) is violated, but the following condition holds:

$$\mathrm{Re}\, \bar{\lambda} a_2 \neq 0,$$

then 0 undergoes a *Chenciner bifurcation* at 0.

A.1 Preliminary transformations

The remainder of this note computes a third order normal form at the origin of the GH-map, following the strategy sketched in the previous subsection.

The system

Consider the family of maps $\Phi_\mu(x) = (\varphi(x, \mu), x_1, x_2, x_3)$, which map the state space $X = \mathbb{R}^4$ into X, with multidimensional parameters $\mu \in P$, where the parameter space P is an open subset of $\mathbb{R}^s$. The evolution map φ is assumed to be of the form:

$$\varphi(x, \mu) = \frac{1}{R}\left((1-n)vx_1 + n(x_1 + g(x_1 - x_2))\right).$$

Here R, v, g are parameters, and n is a function of the form:

$$n = \mathrm{e}^{-x_1^2/\alpha}\tilde{n},$$

with:

$$\tilde{n} = \frac{\mathrm{e}^{-\hat{\beta}(x_1-[x_3+g(x_3-x_4)])^2}}{\mathrm{e}^{-\hat{\beta}(x_1-[x_3+g(x_3-x_4)])^2} + \mathrm{e}^{-\hat{\beta}(x_1-vx_3)^2}},$$

where α and $\hat{\beta} = \beta/(2a\sigma^2)$ are additional parameters. This is the model for nonlinear volatility clustering as presented in GH. Notice that:

$$\mu = (\alpha, \hat{\beta}, v, g, R).$$

Preliminary scaling

An initial state x_0 leads to an orbit $\{x(t)\}_{t=0}^{\infty}$ by iterating the map Φ_μ:

$$x(t+1) = \Phi_\mu\left(x(t)\right).$$

Change to new coordinates $x = \sqrt{\alpha}\,\tilde{x}$. Then the iteration equation changes to:

$$\sqrt{\alpha}\,\tilde{x}(t+1) = \Phi_\mu\left(\sqrt{\alpha}\,\tilde{x}(t)\right),$$

and it follows, by some algebra, that:

$$\tilde{x}(t+1) = \Phi_{\tilde{\mu}}\left(\tilde{x}(t)\right),$$

where the new parameter $\tilde{\mu}$ is equal to:

$$\tilde{\mu} = (1, \alpha\hat{\beta}, v, g, R).$$

Attention may be reduced to the case that $\alpha = 1$, and the parameter μ will be considered to be four-dimensional. In the following, the parameter α as well as the hat of $\hat{\beta}$ are dropped, in order not to overburden the notation.

A.1.1 Linearization around the origin

This note investigates the bifurcations of the origin. For this, the linearization $D\Phi(0)$ of Φ at 0 has to be computed:

$$D\Phi(0) = \frac{\mathrm{d}\Phi}{\mathrm{d}x}(0) = \begin{pmatrix} \frac{1}{2R}(1+v+g) & -\frac{g}{2R} & 0 & 0 \\ 1 & 0 & 0 & 0 \\ 0 & 1 & 0 & 0 \\ 0 & 0 & 1 & 0 \end{pmatrix}$$

Here it is used that for $x = 0$, $n = \frac{1}{2}$. Introduce parameters a and b by:

$$a = \frac{1}{4R}(1 + v + g), \quad \text{and} \quad b = \frac{g}{2R}.$$

The characteristic equation of the matrix then reads:

$$\lambda^2(\lambda^2 - 2a\lambda + b) = 0$$

The root $\lambda = 0$ has multiplicity 2, whereas the other two roots are:

$$\lambda_\pm = a \pm \sqrt{a^2 - b}. \tag{25}$$

Necessary conditions for a Hopf bifurcation

A necessary condition for the occurence of a Hopf bifurcation is that $|\lambda_\pm| = 1$ and $\lambda_\pm \notin \{-1, 1\}$. Equivalently, that:

$$b = 1, \quad \text{and} \quad a^2 - 1 < 0.$$

In terms of the original parameters:

$$g = 2R, \quad \text{and} \quad -6R - 1 < v < 2R - 1.$$

In the following these conditions are assumed to be fulfilled. Let $\lambda = \lambda_+$; note that then $\lambda_- = \bar{\lambda}$.

Eigenvectors

Complex eigenvectors of A are q and $\bar{q} \in \mathbb{C}^4$, given by:

$$q = (1, \bar{\lambda}, \bar{\lambda}^2, \bar{\lambda}^3), \tag{26}$$

satisfying $Aq = \lambda q$, $A\bar{q} = \bar{\lambda}\bar{q}$, and e_3 and e_4, satisfying $A\mathrm{e}_3 = e_4$, $A\mathrm{e}_4 = 0$. Here e_j denotes the j'th unit vector.

A.1.2 Centre space and centre manifold

The (real) subspace spanned by eigenvectors of A with eigenvalues having norm equal to 1 is called the linear *centre* space E^c; eigenvectors to eigenvalues with norm not equal to 1 span the *hyperbolic* space E^h. In the present case, E^c is two-dimensional. It is spanned by linear combinations of q and $\bar{q}$ of the form $zq + \bar{z}\bar{q}$. The space spanned by e_3 and e_4 is the space E^h. The spaces E^c and E^h span together the tangent space of X at zero, which, in the following, will be identified with X.

The Hopf bifurcation can now be studied by reducing the system to a centre manifold of the nonhyperbolic singularity 0. This manifold is tangent to the span of the eigenvectors q and $\bar{q}$. Since every vector $x \in X$ can be written as:

$$x = zq + \bar{z}\bar{q} + y, \tag{27}$$

where $z \in \mathbb{C}$ and $y \in E^h$, the centre manifold can be described by a function $w : E^c \to E^h$, $w = w(z, \bar{z})$, with the property that:

$$w(0,0) = \frac{\partial w}{\partial z}(0,0) = \frac{\partial w}{\partial \bar{z}}(0,0) = 0.$$

Actually, because of the point symmetry of the system, the centre manifold has to be point symmetric as well; consequently, the function w has the property that:

$$w(-z, -\bar{z}) = -w(z, \bar{z}).$$

But then w has to start with third order terms; that is, $w = \mathrm{O}(|z|^3)$. It will suffice to consider the restriction of the dynamics to the linear centre space E^c.

Adjoint eigenvectors

It is convenient to introduce at this point the notion of adjoint eigenvectors. This approach is taken from Kuznetzov (1995).

If the complex inner product $\langle \cdot, \cdot \rangle$ is given by:

$$\langle x, y \rangle = \sum_{i=1}^{n} \bar{x}_i y_i,$$

then there is a unique vector $p \in \mathbb{C}^4$, the *adjoint* eigenvector of q, satisfying:

$$A^T p = \bar{\lambda} p \quad \text{and} \quad \langle p, q \rangle = 1.$$

Here A^T denotes the transpose of A.

Properties
1. $\langle p, \bar{q} \rangle = 0$
2. Any real vector y *satisfies* $\langle p, y \rangle = 0$ *if and only if* $y \in E^h$.

Proof
For the first property, observe that:

$$\lambda \langle p, \bar{q} \rangle = \langle \bar{\lambda} p, \bar{q} \rangle = \langle A^T p, \bar{q} \rangle = \langle p, A\bar{q} \rangle = \bar{\lambda} \langle p, \bar{q} \rangle.$$

Since $\lambda \neq \bar{\lambda}$, the first property follows.

Note for the second property that E^h is the span of (generalized) eigenvectors with eigenvalue having norm not equal to 1. If y is an ordinary eigenvector with eigenvalue μ, then, as above:

$$\lambda\langle p, y\rangle = \langle p, Ay\rangle = \mu\langle p, y\rangle,$$

and since $|\mu| \neq |\lambda| = 1$, it follows that $\langle p, y\rangle = 0$. If y is a generalized eigenvector of A with eigenvalue μ, then there is a $k > 0$ such that $\tilde{y} = A^k y$ is an ordinary eigenvector. Hence:

$$\lambda^k\langle p, y\rangle = \langle p, A^k y\rangle = \langle p, \tilde{y}\rangle = 0;$$

the last equality follows from the previous result. To prove the converse, notice that any vector x can be written as:

$$x = zq + \bar{z}\bar{q} + y,$$

with $y \in E^h$. Assume that $\langle p, x\rangle = 0$. But then the first property and the normalization of p imply together that:

$$0 = \langle p, x\rangle = z\langle p, q\rangle = z,$$

and hence $x = y \in E^h$. ∎

For q given by (26), the vector p is equal to:

$$p = \frac{1}{1-\lambda^2}(1, -\lambda, 0, 0).$$

Projection of the system along eigenvectors

In the new coordinates z, $\bar{z}$ and y introduced in (27), the dynamics, take the form:

$$\Phi(zq + \bar{z}\bar{q} + y) = \zeta(z, \bar{z}, y)q + \overline{\zeta(z, \bar{z}, y)}\bar{q} + \eta(z, \bar{z}, y),$$

where η takes values in E^h. Using the adjoint eigenvector, the projections of Φ on E^c can be computed easily:

$$\begin{aligned}
\zeta(z, \bar{z}, y) &= \langle p, \Phi(zq + \bar{z}\bar{q} + y)\rangle \\
&= \frac{1}{1-\bar{\lambda}^2}(\varphi(zq + \bar{z}\bar{q} + y) - \bar{\lambda}(z + \bar{z})); \qquad (28)\\
\eta(z, \bar{z}, y) &= \Phi(zq + \bar{z}\bar{q} + y) - \zeta q - \bar{\zeta}\bar{q}. \qquad (29)
\end{aligned}$$

Introduce the map Ψ by:

$$\Psi(z, \bar{z}, y) = \left(\zeta(z, \bar{z}, y), \overline{\zeta(z, \bar{z}, y)}, \eta(z, \bar{z}, y)\right).$$

A.2 Normal form computations

Here the normal form computations referred to in subsection A.1.2 are performed. Recall that the map Φ defining the system is of the form $\Phi(x,\mu) = (\varphi(x,\mu), x_1, x_2, x_3)$, with:

$$\varphi(x,\mu) = \frac{1}{R}[(1-n)vx_1 + n(x_1 + g(x_1 - x_2))],$$

where:

$$n = \mathrm{e}^{-x_1^2}\frac{\mathrm{e}^{-\beta u_2}}{\mathrm{e}^{-\beta u_1} + \mathrm{e}^{-\beta u_2}}.$$

Here u_1 and u_2 are of the form:

$$\begin{aligned} u_1 &= (x_1 - v\,x_3)^2, \\ u_2 &= (x_1 - (x_3 + g(x_3 - x_4))^2. \end{aligned}$$

In order to compute the normal form of a Chenciner bifurcation, a Taylor development up to and including fifth order terms of φ is required.

A.2.1 Expansions

Expanding n up to second order yields:

$$\begin{aligned} \frac{\mathrm{e}^{-\beta u_2}}{\mathrm{e}^{-\beta u_1} + \mathrm{e}^{-\beta u_2}} &= \frac{1}{\mathrm{e}^{-\beta(u_1-u_2)} + 1} \\ &= \frac{1}{2 - \beta(u_1 - u_2) + \frac{1}{2}\beta^2(u_1-u_2)^2} + \mathrm{O}(|x|^6) \\ &= \frac{1}{2} + \frac{\beta}{4}(u_1 - u_2) + \mathrm{O}(|x|^4). \end{aligned}$$

Hence, it follows for $n(x)$ that:

$$n(x) = \left(1 - x_1^2\right)\left(\frac{1}{2} + \frac{\beta}{4}(u_1 - u_2)\right) + \mathrm{O}(|x|^6).$$

Substituting this in the expression for φ above, and rearranging terms leads to:

$$\begin{aligned} \varphi(x,\mu) = \frac{1}{R}\Bigg[&vx_1 + (x_1 + g(x_1 - x_2) - vx_1) \\ &\cdot \left(1 - x_1^2\right)\left(\frac{1}{2} + \frac{\beta}{4}(u_1 - u_2)\right) + \mathrm{O}(|x|^7)\Bigg] \end{aligned}$$

A.2.2 Change of variables

The next step is to find an expression of Φ in $(z, \bar{z}, y)$ variables. Note that:

$$(x_1, x_2, x_3, x_4) = (z + \bar{z}, \bar{\lambda} z + \lambda \bar{z}, y_3 + \bar{\lambda}^2 z + \lambda^2 \bar{z}, y_4 + \bar{\lambda}^3 z + \lambda^3 \bar{z})$$

In the new coordinates, the factors of φ have the following form:

$$\begin{aligned} x_1 + g(x_1 - x_2) - v x_1 &= c_0 z + \overline{c_0 z}, \\ 1 - x_1^2 &= 1 - z^2 - 2|z|^2 - \bar{z}^2 \\ \frac{\beta}{4}(u_1 - u_2) &= c_1 z^2 + c_2 |z|^2 + \overline{c_1} \bar{z}^2 + \mathrm{O}(|z||y|), \end{aligned}$$

where the c_j have the following values:

$$c_0 = 1 + g - v - g\bar{\lambda}, \tag{30}$$

$$c_1 = \frac{\beta}{4}(1 - v\bar{\lambda}^2)^2 - \frac{\beta}{4}(1 - (1+g)\bar{\lambda}^2 + g\bar{\lambda}^3)^2, \tag{31}$$

$$c_2 = \frac{\beta}{2}|1 - v\lambda^2|^2 - \frac{\beta}{2}|1 - (1+g)\lambda^2 + g\lambda^3|^2. \tag{32}$$

The projection ζ of Φ along q, given by (28), now reads:

$$\zeta(z, \bar{z}, y) = \lambda z + \frac{1}{1 - \bar{\lambda}^2} \sum_{\substack{m+n=3 \\ m>0, n>0}} \zeta_{mn} z^m \bar{z}^n + \mathrm{O}(|z|^4, |z|^2|y|, |y|^2).$$

The only coefficient which actually has to be computed, ζ_{21}, is given by:

$$\zeta_{21} = c_0(c_2 - 1) + \overline{c_0}\left(c_1 - \frac{1}{2}\right). \tag{33}$$

A.2.3 Normal form transformation

Since $w = \mathrm{O}(|z|^3)$, the dynamics on the centre manifold up to fourth order are given by:

$$\psi(z, \bar{z}) = \zeta(z, \bar{z}, w(z, \bar{z})) = \lambda z + \frac{1}{1 - \bar{\lambda}^2} \sum_{\substack{m+n=3 \\ m>0, n>0}} \zeta_{mn} z^m \bar{z}^n + \mathrm{O}(|z|^5).$$

The form of ψ can be simplified by choosing coordinates appropriately: consider the transformation h, where:

$$z = H(u, \bar{u}) = u + h(u, \bar{u}) = u + \sum_{\substack{m+n=3 \\ m>0, n>0}} h_{mn} u^m \bar{u}^n.$$

In new coordinates, the dynamics $\tilde{\psi}(u, \bar{u})$ have the form:

$$\tilde{\psi}(u, \bar{u}) = \lambda u + \sum_{m+n=3} \left(\frac{\zeta_{mn}}{1 - \bar{\lambda}^2} + \lambda h_{mn} - \lambda^{m-n} h_{mn} \right) u^m \bar{u}^n + \mathrm{O}(|u|^5).$$

Equating to zero as many coefficients of third order terms as possible leads to:

$$h_{30} = -\frac{\zeta_{30}}{\lambda |1 - \lambda^2|^2}, \quad h_{21} = 0, \quad h_{12} = -\frac{\zeta_{12}}{\lambda (1 - \bar{\lambda}^2)^2}, \quad h_{03} = -\frac{\zeta_{03}}{\lambda (1 - \bar{\lambda}^2)(1 - \bar{\lambda}^4)}.$$

Here it is assumed that $\lambda \notin \{1, i, -1, -i\}$. After the transformation, the map ψ reads:

$$\psi(u, \bar{u}) = \lambda u + \frac{\zeta_{21}}{1 - \bar{\lambda}^2} u |u|^2 + \mathrm{O}(|u|^5).$$

Hence, the Hopf bifurcation at 0 is degenerate if:

$$\mathrm{Re}\, \frac{\bar{\lambda} \zeta_{21}}{1 - \bar{\lambda}^2} = \mathrm{Re}\, \frac{\zeta_{21}}{\lambda - \bar{\lambda}} = 0,$$

or, equivalently, if:

$$\mathrm{Im}\, \zeta_{21} = 0. \tag{34}$$

A.2.4 Bifurcation curves

Using equations (25), (30)–(32), (33), (34), and *Mathematica*, the curve of points where the necessary condition for a Chenciner bifurcation (34) is satisfied has been plotted in figure 1 in the main text. This has been done for the case that $R = 1.01$, using the fact the necessary condition for a Hopf bifurcation $g = 2R$ is satisfied for Chenciner bifurcations as well.

References

[1] Arnol'd, V.I., (1983) *Geometric methods in the theory of ordinary differential equations*, Springer.

[2] Arthur, W.B., Holland, J.H., LeBaron, B., Palmer, R. and Taylor, P., (1997) Asset pricing under endogenous expectations in an artificial stock market. In Arthur, W.B., Durlauf, S.N., and Lane, D.A., eds., *The economy as an evolving complex system II*, Redwood City, Addison-Wesley.

[3] Back, A., Guckenheimer, J., Myers, M.R., Wicklin, F.J., and Worfolk, P.A., (1992), DsTool: Computer assisted exploration of dynamical systems, *Notices Amer. Math. Soc.* 39, 303–309.

[4] Bollerslev, T., 1986, Generalized autoregressive conditional heteroscedasticity, *Journal of Econometrics* 31, 307–327.

[5] Björgers, T. and Sarin, R., (1997), Learning Through Reinforcement and Replicator Dynamics, *Journal of Economic Theory* 77, 1–14.

[6] Brock, W.A., (1993) Pathways to randomness in the economy: emergent nonlinearity and chaos in economics and finance, *Estudios Económicos* 8, 3–55.

[7] Brock, W.A., (1997) Asset Price Behavior in Complex Environments, in: Arthur, W.B., Durlauf, S.N., and Lane, D.A., eds., *The Economy as an Evolving Complex System II*, Addison-Wesley, Reading, MA, 385–423.

[8] Brock, W.A., and Hommes, C.H., (1997a) A rational route to randomness, *Econometrica* 65, 1059–1095.

[9] Brock, W.A., and Hommes, C.H., (1997b) Models of complexity in economics and finance, In: Hey, C., Schumacher, J.M., Hanzon, B., and Praagman, C., eds., *System Dynamics in Economic and Financial Models*, Chapter 1, Wiley Publ., pp. 3–41.

[10] Brock, W.A., and Hommes, C.H., (1998), Brock, W.A., and Hommes, C.H., (1998) Heterogeneous beliefs and routes to chaos in a simple asset pricing model, *Journal of Economic Dynamics and Control* 22, 1235–74.

[11] Brock, W.A., and Hommes, C.H., (1999) Rational Animal Spirits, In: Herings, P.J.J., Laan, van der G. and Talman, A.J.J. eds., *The Theory of Markets*, North-Holland, Amsterdam, 109–137.

[12] Brock, W.A., Lakonishok, J. and LeBaron, B., (1992) Simple technical trading rules and the stochastic properties of stock returns, *Journal of Finance* 47, 1731–64.

[13] Broer, H.W., Huitema, G.B., Takens, F., and Braaksma, B., (1990) Unfoldings and bifurcations of quasi–periodic tori, *Memoirs of the AMS* **83**

[14] Chenciner, A., (1985) Bifurcations de points fixes elliptiques. I. Courbes invariantes, *IHES–Publications mathématiques* 61, 67–127.

[15] Chenciner, A., (1985) Bifurcations de points fixes elliptiques. II. Orbites periodiques et ensembles de Cantor invariants, *Inventiones mathematicae* 80, 81–106.

[16] Chenciner, A., (1988) Bifurcations de points fixes elliptiques. III. Orbites périodiques de "petites" périodes et élimination résonnante des couples de courbes invariantes, *IHES–Publications mathématiques* 66, 5–91.

[17] Chiarella, C., (1992) The dynamics of speculative behaviour, *Annals of operations research* 37, 101–123.

[18] Chiarella C., He X.-Z., (2000) Heterogeneous Beliefs, Risk and Learning in a Simple Asset Pricing Model. *Computational Economics*, forthcoming.

[19] Doedel, E.J., Champneys, A.R., Fairgrieve, T.F., Kuznetsov, Yu.A., Sandstede, B., and Wang, X., (1998) AUTO 97: Continuation and Bifurcation Software for Ordinary Differential Equations (with HomCont). http://indy.cs.concordia.ca/auto/main.html

[20] De Long, J.B., Shleifer, A., Summers, L.H., and Waldmann, R.J., (1990) Noise trader risk in financial markets, *Journal of Political Economy* 98, 703–738.

[21] Engle, R.F., (1982) Autoregressive conditional heteroscedasticity with estimates of the variance of United Kingdom inflation, *Econometrica* 50, 987–1007.

[22] Evans, G. and Honkapohja, S., (1998) Learning Dynamics, in Taylor, J.B. and Woodford, M., *Handbook of Macroeconomics*, Elsevier, Amsterdam.

[23] Farmer, J.D., 2000, Market force, ecology and evolution, *Journal of Economic Behaviour and Organization*, forthcoming.

[24] Frankel, J.A. and Froot, K.A., (1988) Chartists, Fundamentalists and the Demand for Dollars, *Greek Economic Review* 10, 49–102.

[25] Friedman, M., (1953) The case of flexible exchange rates, In: *Essays in positive economics*, Chicago, Univ. Chicago Press.

[26] Gaunersdorfer A., (2000a) Endogenous fluctuations in a simple asset pricing model with heterogeneous beliefs, *Journal of Economic Dynamics and Control* 24, 5–7: 799-831.

[27] Gaunersdorfer A., (2000a) Adaptive Beliefs and the Volatility of Asset Prices, *Working Paper*, University of Vienna.

[28] Gaunersdorfer A. and Hommes C.H., (2000), A Nonlinear Structural Model for Volatility Clustering, *SFB Working Paper* No. 63, University of Vienna and Vienna University of Economics and Business Administration, and CeNDEF Working Paper.

[29] Grandmont, J.-M., (1998) Expectations Formation and Stability in Large Socio-Economic Systems. *Econometrica* 66, 741–81.

[30] Granger, C.W.J. and Teräsvirta, T., (1999) A simple nonlinear time series model with misleading linear properties. *Economic Letters* 62, 161–165.

[31] Guckenheimer J. and Holmes P., (1986) *Nonlinear oscillations, dynamical systems, and bifurcations of vector fields*, Springer, New York.

[32] Herman M., (1979) Sur la conjugaison différentiable des difféomorphismes du cercle à des rotations, *Publ. Math IHES* 49, 5–234.

[33] Hommes C.H., (1992) Periodic, Quasi-Periodic and Chaotic Dynamics in a Simple Macro Model with Hicksian Nonlinearities, In: Feichtinger G., ed., *Dynamic and Economic Models and Optimal Control*, Elsevier Science Publishers.

[34] Hommes C.H., (2000) Financial Markets as Nonlinear Adaptive Evolutionary Systems, *CeNDEF Working Paper*, University of Amsterdam.

[35] Jacobson, M.V., (1981) Absolutely continuous invariant measures for one-parameter families of diffeomorphisms, *Comunications in Mathematical Physics* 81, 39–88.

[36] Kirman, A., (1991) Epidemics of opinion and speculative bubbles in financial markets, In M. Taylor (ed.), *Money and financial markets*, Macmillan, London.

[37] Krauskopf, B. and Osinga, H.M., (1998) Investigating torus bifurcations in the forced Van der Pol oscillator, *IMA Vol. Math. Appl.*, Springer-Verlag.

[38] Kuznetsov, Y.A., (1998a) *Elements of Applied Bifurcation Theory* (2^{nd} ed.), Springer Verlag, New York.

[39] Kuznetsov, Y.A., (1998b) CONTENT – Integrated environement for analysis of dynamical systems. Tutorial. ftp://ftp.cwi.nl/pub/CONTENT/

[40] LeBaron, B., (2000) Evolution and time horizons in an agent based stock market, *Working paper Brandeis University*, June 2000.

[41] LeBaron, B., Arthur, W.B. and Palmer, R., (1999), Time series properties of an artificial stock market, *Journal of Economic Dynamics and Control* 23, 1487–1516.

[42] Lux, T., (1995) Herd Behavior, Bubbles and Crashes, *The Economic Journal* 105, 881–896.

[43] Lux, T. and Marchesi, M., (1999a) Scaling and criticality in a stochastic multi-agent model of a financial market, *Nature* 397, February 1999, 498–500.

[44] Lux, T. and Marchesi, M., (1999b) Volatility clustering in financial markets: a micro-simulation of interacting agents, *International Journal of Theoretical and Applied Finance*, in press.

[45] Mandelbrot, B., 1963, The variation of certain speculative prices, *Journal of Business* 36, 394–419.

[46] Mora, L., and Viana, M., (1993) Abundance of strange attractors, *Acta Mathematica* 171, 1–71.

[47] Moser, J., (1973) *Stable and Random Motions in Dynamical Systems*, Princeton University Press.

[48] Newhouse, S., Palis, J. and Takens, F., (1983) Bifurcations and stability of families of diffeomorphisms, *IHES–Publications mathématiques*, 5–72.

[49] Palis, J. and Takens, F., (1993) *Hyperbolicity and sensitive chaotic dynamics at homoclinic bifurcations*, Cambridge University Press.

[50] Pomeau, Y. and Manneville, P., (1980) Intermittent transition to turbulence in dissipative dynamical systems, *Communications in Mathematical Physics* 74, 189–197.

[51] Pintus, P., Sands, D., and Vilder, de R., (2000) On the transition from local regular to global irregular fluctuations, *Journal of Economic Dynamics and Control* 24, 247–272.

[52] Sargent, Thomas J., (1993) *Bounded Rationality in Macroeconomics*, Clarendon Press, Oxford.

[53] Sargent, Thomas J., (1999) *The Conquest of American Inflation*, Princeton University Press, Princeton.

[54] Timmermann, A., 1993, How learning in financial markets generates excess volatility and predictability in stock prices, *Quarterly Journal of Economics* 108, 1135–1145.

[55] Timmermann, A., 1996, Excess volatility and predictability of stock prices in autoregressive dividend models with learning, *Review of Economic Studies* 63, 523–557.

[56] Vilder, de R.G., (1996) Complicated dynamics in a two-dimensional overlapping generations model. *Journal of Economic Theory* 71, 416–442.

[57] Zeeman, E.C., (1974) The unstable behavior of stock exchange, *Journal of Mathematical Economics* 1, 39–49.